Recent Advances in the Development of Nanocarbon-Based Electrocatalytic/Electrode Materials for Proton Exchange Membrane Fuel Cells: A Review

Adelina A. Zasypkina [1], Nataliya A. Ivanova [1], Dmitry D. Spasov [1,2], Ruslan M. Mensharapov [1], Matvey V. Sinyakov [1,3] and Sergey A. Grigoriev [1,2,4,5,*]

[1] Department of Electrochemical and Hydrogen Technologies, National Research Center "Kurchatov Institute", Akademika Kurchatova sq., 1, 123182 Moscow, Russia; adelinazasypkina@yandex.ru (A.A.Z.); ivanovana.1989@mail.ru (N.A.I.); spasovdd@outlook.com (D.D.S.); ruslan.mensharapov@gmail.com (R.M.M.); mmatveimatvei4@gmail.com (M.V.S.)

[2] Department of Chemistry and Electrochemical Energy, National Research University "Moscow Power Engineering Institute", Krasnokazarmennaya st., 14, 111250 Moscow, Russia

[3] Department of Isotope Technology and Hydrogen Energy, Institute of Modern Energetics and Nanotechnology, D. Mendeleev University of Chemical Technology of Russia, Miusskaya sq., 9, 125047 Moscow, Russia

[4] HySA Infrastructure Center of Competence, Faculty of Engineering, North-West University, Potchefstroom 2531, South Africa

[5] Laboratory for Aliphatic Organoboron Compounds, A.N. Nesmeyanov Institute of Organoelement Compounds, Russian Academy of Sciences, Vavilova st., 28, 119991 Moscow, Russia

* Correspondence: grigoryevsa@mpei.ru

Abstract: The global issue for proton exchange membrane fuel cell market development is a reduction in the device cost through an increase in efficiency of the oxygen reduction reaction occurring at the cathode and an extension of the service life of the electrochemical device. Losses in the fuel cell performance are due to various degradation mechanisms in the catalytic layers taking place under conditions of high electric potential, temperature, and humidity. This review is devoted to recent advances in the field of increasing the efficiency and durability of electrocatalysts and other electrode materials by introducing structured carbon components into their composition. The main synthesis methods, physicochemical and electrochemical properties of materials, and performance of devices on their basis are presented. The main correlations between the composition and properties of structured carbon electrode materials, which can provide successful solutions to the highlighted issues, are revealed.

1. Introduction

The commercial development of the proton exchange membrane fuel cell (PEMFC) market relies on overcoming several challenges. One significant limitation of fuel cell efficiency is the slow oxygen reduction reaction (ORR) that occurs at the cathode [1–3]. To accelerate the ORR and improve its efficiency, it is necessary to use platinum group catalysts; thus, pure platinum or platinum on a carbon support is used to increase the active catalyst surface [4]. Usually, carbon black is used as a platinum particle support due to its availability and low cost, as well as appropriate values of specific surface area and electrochemical characteristics [5–7].

It also remains important to reduce the degradation rate of membrane electrode assembly (MEA) components, particularly catalysts and their supports [8]. Catalyst degradation can occur either mechanically through membrane damage or through electrochemical

reactions during the PEMFC operation. Thus, when water is generated in a fuel cell as a product of an electrochemical reaction, it stagnates in gas diffusion layers (GDLs), bipolar plates (BPs), or catalytic layers (CLs) [9]. This phenomenon negatively affects the mass transfer of reagents and, over time, leads directly to degradation of the above FC components and deterioration of the device output characteristics [10–12]. When humidity is too low, the proton exchange membrane changes its geometry and dimensions [13], leading to mechanical failure of the CL being in direct contact with the membrane [14,15].

Deterioration in FC performance is also caused by various mechanisms of catalytic layer degradation, which occur under the influence of electrical potential, elevated temperature, and humidity [16,17]. Carbon corrosion is the main cause of catalyst degradation [18]. When the potential reaches 0.207 V (relative to a standard hydrogen electrode), the oxidation process of the carbon support begins [19]. However, in low-temperature hydrogen FCs, this process is inhibited by the reduced temperature [20]. The process is accompanied by the spontaneous agglomeration of platinum particles and their recondensation, or Ostwald ripening (any increase in the number of catalyst particles leads to a decrease in the active surface and, consequently, a decrease in the electrochemical surface area (ESA)), as well as their separation and dissolution (Figure 1) [21–24]. In this case, platinum accelerates the carbon-oxidation reaction [25]. The degradation mainly occurs during the ORR taking place at the cathode, when the reduction intermediates and oxygen itself start affecting the catalytic layer [26].
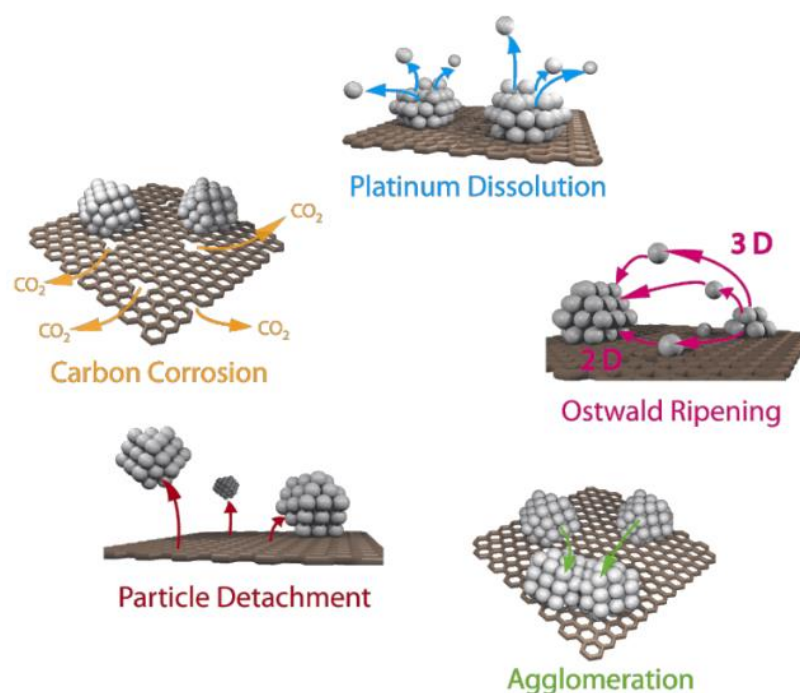
Figure 1. Simplified representation of suggested degradation mechanisms for platinum particles on a carbon support in fuel cells [22]. Copyright 2014, Beilstein Institute.

The most promising and investigated method for tackling the problem of CL degradation due to gradual oxidation of the carbon support is the use of structured materials as supports. Due to the original structure of graphite, it is possible to synthesize quite complex and diverse carbon nanomaterials on its basis. These include all types of graphene structures and their derivatives: carbon nanotubes (CNTs) and nanofibers (CNFs), graphene nanosheets, graphene oxides (GOs), reduced graphene oxides (rGOs), arrays of nanotubes, aligned and non-aligned, as well as graphene aerogels, honeycombs, spheres, and others [27–33].

Graphene and its various configurations possess excellent physical and chemical properties, including a large specific surface area, high electrical and thermal conductivity,

durability, chemical resistance, and mechanical strength [34–36]. The use of complex carbon structures in CL leads to a more uniform distribution of catalytic particles on the surface and hence high electrochemical activity, gas permeability, and electrical conductivity [37–40]. At the same time, due to the appearance of micro- and macro-pores as a result of the specific packing of graphene particles, the water balance of FC is improved [30]. These materials are highly suitable and promising for use as electrocatalytic and electrode materials in fuel cell components, such as CLs, microporous layers (MPLs), and GDLs.

The current trends in the development of carbon nanomaterials technology are aimed at improving the methods for synthesizing materials with specified properties and expanding their applications, including electrochemical energy storage and conversion (supercapacitors, lithium-ion batteries, electrolysis systems (hydrogen evolution reaction (HER)), and fuel cells (hydrogen oxidation reaction (HOR) and ORR)). The growth in demand and applications of electrochemical current sources has led to a rapid development of research in the synthesis and properties of these structures, which have a favorable impact on the efficiency and durability of device components. The abundance of published materials in various research areas necessitates their analysis and systematization to address the challenges currently facing the PEMFC industry. This review will focus on these challenges and consider studies of the properties of electrocatalyst support materials. These properties include high conductivity, surface area, the presence of functional groups that improve metal deposition, and the durability of materials during operation. On the other hand, the decline in the number of studies on the properties of electrocatalysts highlights the problem of developing an effective catalytic layer that provides the hydrophilic/hydrophobic balance and optimal porosity for high transport efficiency. The main focus of this review is on systematizing properties and selecting the optimal material structure in terms of efficiency in the FC electrode (cathode).

2. Graphene Structures

2.1. Graphene Nanosheets

The structure of graphene is represented as one or more layers of sheets of one-atom-thick sp^2 hybridized carbon. Currently, there are many different techniques for making graphene, as each technique produces nanosheets with unique physical and chemical characteristics required in a particular field. Methods for producing graphene include physical or chemical layering, epitaxial growth through chemical vapor deposition (CVD), unzipping of carbon nanotubes through electrochemical, chemical, or physical methods, and reduction of sugars such as glucose or sucrose [38]. Graphene is the fundamental precursor of all graphitic carbon structures, including carbon nanotubes, nanofibers, spheres, and other nanostructures. The approximate thickness of one layer of graphene is 0.345 nm [27], which has a positive effect on the uniformity of the distribution of catalytic particles on it and the increase of active sites. Graphene nanosheets also have many different derivatives used as catalyst supports in PEMFCs, which are graphene oxides as well as graphene doped with heteroatoms.

For carbon materials, functional groups are important in the synthesis of platinum catalysts. They serve as adsorption sites for the nucleation of small Pt particles, resulting in a uniform distribution of Pt on the carbon support [41]. The capacitance of the double-layer electrode with platinum deposited on carbon depends on the surface morphology and the type of functional groups fixed in the support [42]. The smaller average Pt particle size is a result of the finer catalyst particle size, which indicates the existence of more anchoring sites on the graphene. This provides better dispersion of Pt particles [43]. Compared to spherical carbon particles, the planar structure of graphene facilitates the uptake of oxygen functional groups, mainly at the edges of graphene sheets [41].

While surface defects have been found to improve the activity of graphene-based electrocatalysts in ORR and enhance Pt dispersion, long-term observations have also revealed that these properties can result in carbon corrosion due to unsaturated valences and free s-electrons [44], as well as the adverse effects of highly concentrated s-electrons.

Functional groups also decrease electrical conductivity and increase water affinity. This may make it more difficult to remove water from the fuel cell, which can lead to substrate corrosion and primarily Pt dissolution.

The addition of graphene nanosheets to the MPL improves the performance of PEMFC in both low- and high-humidity conditions [45]. The addition of graphene to MPL has been found to decrease membrane dehydration in low humidity conditions. Additionally, it has been observed to decrease liquid water saturation at the catalyst layer–GDL interface in high-humidity conditions [46]. This is due to the presence of a large number of micropores, which contribute to the retention of water needed to wet the membrane and electrolyte in the catalyst layer. Graphene exhibits a uniform distribution of micropores and small mesopores. This characteristic can enhance performance at high relative humidity and current densities by facilitating simultaneous capillary absorption of liquid water to reduce cathode flooding and improve the diffusion of reactants into the catalyst bed [47]. Graphene nanoplatelets exhibit dense horizontal stacking of graphene flakes in MPL, which leads to a reduction in pore volume. However, this effect results in a slight increase in the MPL wetting angle and therefore enhances hydrophobicity. In this case, there are fewer pathways for water removal from the surface, which hinders air flow towards the through-plane. As a result, through-plane permeability and efficiency decrease with increasing graphene content [45,48]. The electrical conductivity of graphene nanoplatelets is significantly affected by the number of graphene layers, lateral size, and material purity [49]. The resistivity measurements indicate that the inclusion of just 30% graphene in MPL significantly enhances the electronic conductivity of the layer, resulting in a 20% reduction in resistivity compared to a conventional carbon black-based MPL [45].

When comparing Pt catalysts based on graphene sheets and carbon black [50], this study found a three-fold increase in the ORR mass activity for graphene. This was attributed to higher charge transfer rates or lower binding energy with reactive adsorbates. The increase in ESA is due to the smaller average particle size of the Pt particles. This results in the presence of a disordered structure, more electroactive sites, and the ability to form more three-phase boundaries. Additionally, there are strong metal-support interactions and high dispersion of the nanoparticles [51–53]. Reducing the size of catalytic particles also leads to a higher utilization of said particles [50]. However, graphene-based catalysts generally exhibit superior degradation resistance and stability, which can be attributed to the presence of functional groups. Graphene may contain functional groups such as N, O, and S, depending on the synthesis or functionalization method used. During catalyst synthesis, active metal particles replace certain groups in the graphene structure. This significantly strengthens atomic bonding and improves catalyst degradation stability [27,41,46]. Electrochemical studies have shown that the catalytic activity and stability of graphene-based bimetallic catalysts are significantly enhanced by the addition of a secondary metal [54]. The initial decrease in activity is likely caused by the dissolution of subsurface and/or surface atoms of the second metal and/or Pt, followed by the re-formation of a stable number of electrons transferred per oxygen molecule for all catalysts [51].

Although graphene nanosheets have advantages, they can negatively affect MEA functioning. Therefore, when CVD graphene is used as a catalyst support deposited on GDLs, mass transfer limitations are observed at low polarization voltages when the current density suddenly decreases [55]. The high graphene content in the catalyst caused agglomeration, which characterizes the inefficiency of using such a layer to periodically remove water generated at the cathode [56]. The electrochemical performance deterioration is caused by mass transfer issues, which can be attributed to the presence of mesopores and densely stacked graphene sheets [45].

2.2. Graphene Oxide and Reduced Graphene Oxide

Graphene oxide is a single-layer sheet-like structure with functional groups. Oxygen groups such as hydroxyl and epoxy groups are located on the basal planes, while other groups, such as carboxy, carbonyl, phenol, etc., are mainly based on the leaf edges. These

oxygen-containing groups and defects alter its physicochemical properties. GO is highly hydrophilic and disperses uniformly in water, making it an excellent electrode material [57]. However, the electrical conductivity of GO is lower than that of graphene because of the functional groups present on its surface [27].

Reduced graphene oxide is obtained in several steps, first from graphite to GO by thermal or chemical oxidation and then by reduction to reduced graphene oxide. Several methods exist for synthesizing GO, including the Brodie, Staudenmaier, and Hummers methods and their modified and improved variants [58,59].

The reduced graphene oxides have a more mesoporous structure with fewer micropores compared to graphene. They are aggregate friable aggregations of lamellar particles forming slit-like pores [60]. This is evidenced by characteristic sorption isotherms with a hysteresis loop, which is associated with capillary condensation occurring in mesopores, as well as with limiting absorption in the range of high P/P_0 (the ratio of pressure in the system to the condensation pressure) [61,62]. There is also a sufficient number of macropores, which play the role of gas transport channels in the structure. Thus, the specific porous structure of rGO with multiple mesopores and open and interconnected channels promotes rapid diffusion of fuel to the active Pt sites [62]. During the synthesis of metal particles onto the support, the doping process causes a decrease in surface area. However, the resulting catalysts maintain their original mesoporosity, which is a crucial aspect in the fabrication of catalysts for PEMFCs [62]. Gold nanoparticle catalysts supported on reduced graphene oxide (AuNP/rGO) with a high specific surface area and mesoporous structure, featuring a narrow and regular pore size distribution, have been successfully fabricated [63].

It is demonstrated in Ref [64] that rGO can serve as a capacitive material when incorporated into a catalytic layer along with platinum particles. Scanning electron microscopy (SEM) images of the rGO/Nafion layer on carbon paper revealed a homogeneous three-dimensional porous structure of rGO sheets (Figure 2a–c). The pore diameter of the rGO/Nafion layer was in the range of 0.7 to 9 μm, which was approximately 10–100 times longer than the free path length of O_2. This could facilitate the mass transfer of O_2. Elemental mapping images of the rGO/Nafion thin layer (Figure 2d–g) showed the presence of uniformly distributed S and F, which can be explained by the technique used to obtain the original graphene that underwent subsequent oxidation. After atomization of the catalytic ink, Pt/C/Nafion aggregated on the inner wall of the pores of the rGO sheets. Despite the inaccuracy of determining pore diameter from SEM images, the authors noted maintaining a porous structure while the pore diameter decreased.

The presence of functional groups on the surface of GO and rGO is clearly visible when GO is examined by Fourier-transform infrared spectroscopy (FTIR), the results of which are shown in Figure 3. In [65], functional groups related to graphite and rGO powders were investigated, from which the effect of oxidation on the properties of graphene can be determined. The graphite spectra in Figure 3 show a broad band in the 3000–3600 cm^{-1} region representing the valence vibration due to the presence of a hydroxyl group (O-H vibration). The spectrum shows typical peaks indicating oxygen-containing groups: 1919.77 cm^{-1} for C=O (carbonyl/carboxyl) and a broad band at 1000–1340 cm^{-1} for carboxy C-O, epoxy C-O, and alkoxy-C-O. The peak at 1619.81 cm^{-1} corresponds to the planar vibrations of the aromatic compound C=C, at 2112.61 cm^{-1} for C:O, and at 2271.16 cm^{-1} for CH. The IR spectra of rGO showed a significant decrease in the bands corresponding to the O-H and C:O groups, while the peaks corresponding to the epoxy and alkoxy C=O groups and C-H groups disappeared completely, as shown in Figure 3.

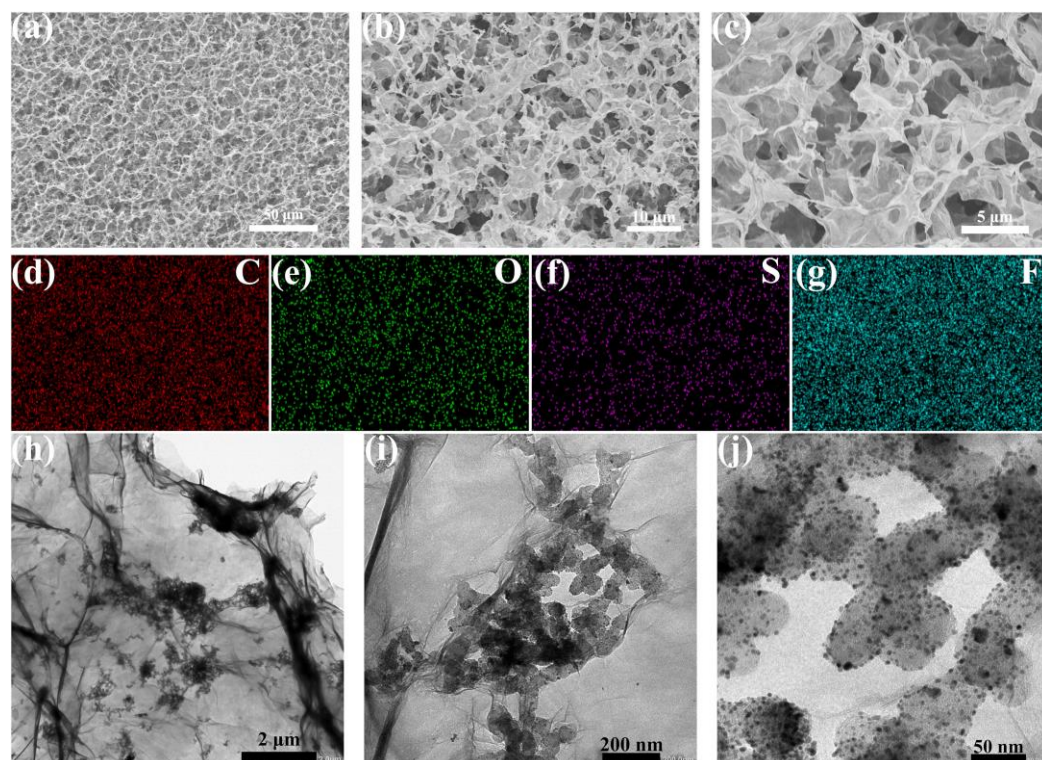**Figure 2.** (**a**–**c**) SEM images of the rGO/Nafion layer. (**d**–**g**) Element mapping images of C, O, S, and F based on (**a**). (**h**–**j**) Transmission electron microscopy (TEM) images of the rGO sheets adsorbed Nafion and Pt/C particles in the rGO–NF–Pt electrode [64]. Copyright 2023, Elsevier.
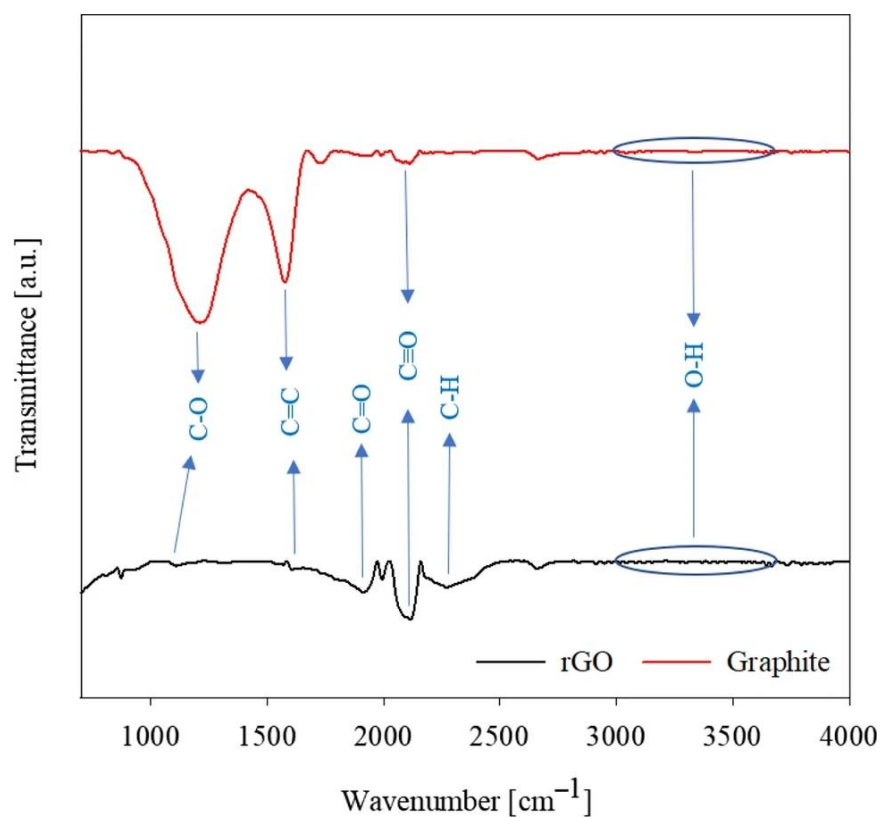

Figure 3. FTIR analysis related to graphite and rGO [65]. Copyright 2023, Springer.

The reduced graphene oxides have a structure between pure graphene and graphene oxide [66]. During chemical and thermal reduction, the quantity of oxygen-containing functional groups is considerably decreased. This is explained by the fact that the p-conjugated structure of graphene is essentially restored in the synthesized rGO, with the opening of epoxy rings having a significant influence on this situation. It has also been found that the thin nanolayer of rGO folds together to form a thick bulk structure due to the presence of strong van der Waals forces between each layer [67]. The reduction of oxygen-containing functional groups increases the hydrophobicity of rGO-based samples owing to the reduction in oxygen concentration [61], but due to the high porosity of these samples, this cannot affect the electrical conductivity [65].

Under reaction conditions, the spectra of the graphene-based catalysts indicate partial removal of major functional groups from GO compared to the original graphene oxide. The functional groups likely served as anchoring sites for metallic platinum ions during the reduction reaction, promoting the production of metal nanoparticles that are distributed on the rGO sheets [62]. The embedding of metal nanoparticles in the support structure and their interaction with it have a positive effect on the chemical and mechanical stability of the catalyst. This prevents the development of agglomeration processes and the migration of catalyst particles.

In [65], the effect of adding rGO and graphite to MPL by pressing on various properties of the GDL for which Toray carbon paper was used is studied. The study has demonstrated that MPLs based on rGO have a smooth and planar morphology as well as higher in-plane electrical resistivity compared to graphite-based MPLs. However, the rGO-based MPLs have lower roughness than the graphite-based MPLs. Replacing graphite with rGO increases the wetting angle, porosity, and permeability of the samples. And graphite-based MPLs have lower resistivity.

The catalytic activity of rGO-based catalysts is high due to the presence of a larger number of active sites that more effectively adsorb reactants during the catalytic ORR process [41]. The reduced graphene oxide itself can serve as electroactive sites and also reduce the ion diffusion pathway, which also results in high electrical conductivity and better electrical contacts [63].

The accelerated MEA degradation test results indicate that Pt/rGO exhibits nearly twice the degradation resistance compared to other materials [62]. Stronger electronic interactions between Pt nanoparticles and graphene support result in this effect. The metal-substrate interaction is strengthened, as shown by the negative shift of the Pt 4f binding energy in the X-ray photoelectron spectroscopy (XPS) spectra. This suggests that electrons are transferred from the carbon supports to Pt [39]. The resistance to degradation is also affected by the slower corrosion of the support, which is caused by fewer disordered sites for graphene derivatives.

The current density value in the electrooxidation of methanol using a multicomponent core-shell catalyst based on rGO is approximately four times higher than that of similar catalysts based on amorphous carbon support and approximately six times higher than that of Pt/C [68]. These results suggest that such an electrocatalyst exhibits high volumetric activity, high stability, and high resistance to CO poisoning, thus reducing the platinum loading in PEMFCs. The use of synthesized Pt/rGO material as a cathode catalyst increased the maximum specific power by up to 17% and significantly improved fuel cell performance, particularly at high current densities [39]. The efficiency of MEA depends on the catalyst activity and ESA, as well as the layer structure and thickness. These factors significantly affect the mass transfer of reactants and can cause a deterioration in load transfer resistance due to an imbalance in the three-phase boundary. It is important to maintain a balance at the three-phase boundary to ensure optimal efficiency [66]. To address this issue, it has been suggested that a mixture of graphene with either carbon black or CNT could be used [41]. The rGO–Vulcan mass ratio of 75:25 provides the highest ESA [69] as well as its lowest loss.

Although graphenes and their oxides have advantages as MEA components, such as high catalytic and electrochemical activity, stability, and degradation resistance, there is an issue with mass transfer of gas reagents and their products during cell operation, which significantly affects the efficiency of the PEMFC operation. Therefore, the formation of catalytic layers and MPL based on graphene and its oxides, which meet the requirements for structure and porosity and ensure efficient operation of the device, remains a significant challenge.

3. Carbon Nanotubes

Carbon nanotubes are used as supports for FC catalysts. They can be single-walled or multi-walled and can form arrays, including oriented ones, depending on the synthesis methods and application purposes. Several techniques are currently employed for the synthesis of CNTs, with the most prevalent being electric arc evaporation of graphite electrodes, laser ablation of graphite targets, and catalytic pyrolysis of gaseous hydrocarbons. CNTs are two-dimensional hexagonal tubular structures formed by a single layer of graphene with strong meshes of sp^2-hybridized atoms. CNTs can be 0.5–20 nm in diameter and up to hundreds of micrometers in length [70]. Due to their tubular structure, CNTs have a large specific surface area, which is one of the main advantages for the application of this support in PEMFCs [71]. In addition, the material's mechanical properties, such as its modulus of elasticity and hardness, are improved compared to those of other structured materials [72].

For single-walled CNTs (SWCNTs), each carbon atom carries a pair of π-electrons that do not participate in bond formation. These electrons form a conjugated π-electron cloud along the entire length of the CNT. Multi-walled carbon nanotubes (MWCNTs) consist of several concentric tubes of coiled graphene sheets arranged one inside the other, similar to a matryoshka doll. In certain instances, a multi-walled nanotube structure can be created by twisting a single graphene sheet around itself, resembling a sheet of parchment. For multi-walled CNTs, the carbon atoms within each layer are connected by strong covalent bonds. The multi-walled CNT layers are connected by weak van der Waals interactions, resulting in a layer-to-layer distance similar to that of graphite, approximately 3.4 Å.

The size of catalyst particles is a critical factor that determines the electrocatalytic activity and durability of the platinum electrocatalyst used in fuel cells. The electrochemical and catalytic activity of Pt nanoparticles synthesized on CNTs is improved due to their smaller size and uniform distribution. This is because the increased number of active sites and higher electrical conductivity promote rapid electron movement in the support [73–75]. The catalysts based on MWCNTs exhibited a positive shift in Pt $4f_{7/2}$ binding energies compared to crystalline Pt. The extent of this shift was found to be related to the size of the Pt nanoparticles on the MWCNTs; specifically, the smaller the nanoparticles, the more positive the shift [74]. This effect is reported to be attributed to initial state effects, such as changes in the coordination number of the atom or charge transfer effects [76]. Alternatively, the shift may be caused by end-state effects, such as relaxation effects [77]. This effect also makes it possible to significantly reduce the platinum catalyst loading. The use of nanotubes as a support for platinum particles enables high dispersibility, similar to that of graphene and its reduced oxide.

The synthesized CNTs initially exhibit various structural defects, including surface indentations, metal impurities, and amorphous carbon. These defects are evident in the XPS spectroscopy, which indicates the presence of sp^3-hybridized carbon [78]. The graphitization index (GI) indicates the amount of sp^2 carbon and is calculated from the interplanar distances obtained from X-ray diffraction analysis (XRD). Increasing the GI enhances the strength of p-sites (sp^2-hybridized carbon). These sites function to attach Pt particles to the support material and improve metal interactions with the support material [79]. The presence of structural defects in the grown MWCNTs is advantageous for achieving a more uniform deposition of Pt nanoparticles with reduced loading control due to the increased binding energy between MWCNTs and Pt nanoparticles and their good distribution [80]. The presence of C-O and C=O IR peaks in Pt/MWCNTs catalysts is attributed to their existence in the structure of carbon nanotubes used as a substrate

for Pt nanostructures. Oxidized particles may form during the thermal decomposition of acetylene in the presence of trace amounts of oxygen in a CVD furnace [74].

To preserve the structure of CNTs during the synthesis of catalysts, an impregnation method is used. Acids and salts of metal precursors are most commonly used as precursors. Electrodes produced using this method exhibit greater stability as a result of the strong adhesion between the metal particles and the nanotubes [81,82].

The electrocatalytic activity of three-dimensional porous MWCNT electrodes was tested on a rotating disc electrode setup. At 0.9 V, the results indicate that Pt has a higher current in ORR per ESA and an extended kinetic current region, which remain stable after the durability stress test (DST). This phenomenon is also observed for ultra-low Pt loadings up to 14.2 $\mu g/cm^2$ [74]. A comparison of the performance of catalysts in PEMFC with 0.1 mg/cm^2 Pt loading on the cathode and of the impedance data showed that the Pt/CNT catalyst was the most active one [83]. Electrochemical measurements using cyclic voltammetry (CV) and linear sweep voltammetry (LSV) showed that Pt/CNT exhibited higher mass and specific activity compared to commercial Pt nanoparticles deposited on graphitized carbon (Pt/C) [84,85]. The selective activity towards HOR, improved by 30% compared to commercial samples, was the main indication of catalyst retention in SWCNTs [75]. It is also possible to increase catalytic activity by using bimetallic catalysts on MWCNT, for example, PtNi/MWCNT. The ORR mass activity of such a catalyst is 1.4 times higher than that of a conventional commercial electrocatalyst [86].

The use of CNTs instead of carbon black provides a high utilization rate of Pt in MEA [83] compared to the Pt/C catalyst. The higher use of platinum characterizes the higher number of Pt active sites and three-phase boundaries in the applied catalysts [79], and hence their high catalytic activity [87].

Carbon corrosion proceeds during a potential cycling test through the oxidation of functional groups of carbon support to CO_2 and CO and is enhanced in the presence of Pt nanoparticles [86]. CNTs in this case are less susceptible to corrosion than carbon black, even though the platinum particles are highly active. The main reason for the higher durability is the chemical inertness of the structured material [86]. ESA losses observed during DST are up to 40%, which is an excellent indicator of electrochemical resistance [79]. A study of the degradation properties of CNT-based catalysts under fuel cell operating conditions showed more stable behavior than with commercial Pt/C, including after 10,000 startup/shutdown cycles [84]. However, destruction of the electrode structure is observed due to the formation of larger pores in the catalytic layer with a significant thickness as a result of support corrosion [88]. The high thermal stability of these materials also enhances their degradation resistance. CNT-based catalyst synthesis can also significantly reduce electrode wear and improve long-term stability during potential cycling due to resistance to Pt agglomeration during ORR/HOR [75].

During tests on a fuel cell, a 15 μm thick CNT MPL was found to increase the peak power density of the device by 50.9% when air was supplied at the cathode and by 20.9% when pure oxygen was supplied at the cathode, compared to a conventional PEMFC [89]. When CNTs are used as catalyst support, the MEA also exhibits a high current density and electron transfer rate up to 50% higher than that of Pt/C [75,84,85]. Electrochemical impedance analysis revealed that the CNT MPL effectively reduced the charge transfer resistance. This improvement was attributed to the enhanced reaction kinetics and mass transfer through MPLs [86]. The MEA performance was significantly improved by adding a single-walled carbon nanotube nonwoven layer between the gas diffusion substrate and the hydrophobic MPL. The excellent electrical conductivity and rational pore structure of the material result in improved wettability and water-holding capacity of MEA, leading to enhanced performance under low humidity conditions [90]. Also, the porous structure of the electrode when CNTs are added to the electrode composition can improve the gas transfer and water drainage characteristics, which helps to improve the FC performance [91].

Vertically Aligned CNTs

Vertically aligned CNTs (VACNTs) are basically arrays of parallel-oriented nanotubes grown on a substrate (Figure 4b). In this case, nanotubes can be either single-walled or multi-walled. The synthesis of CNTs is carried out by the catalytic decomposition of hydrocarbons (for example, methane). The desired morphological and physical properties of nanotubes are achieved by applying different variations [92]. The performance of CNTs is also affected by a number of other factors, such as the material of the substrate used during synthesis, the tube growth catalyst used, and how it is applied [93–95]. The use of VACNTs as an electrocatalyst support greatly influences the degradation stability and performance of PEMFCs due to the peculiarity of their formation. The synthesis of aligned tubes directly on the substrate results in enhanced adhesion of the microporous and catalytic layers [96]. VACNTs possess a developed surface that facilitates the deposition of nanometer-sized platinum particles and prevents their agglomeration. This reduces the loading of expensive catalysts and increases their efficiency. When a film of aligned CNTs is used as an FC cathode, it increases the current density, performance, and electrocatalytic activity compared to a Pt/non-aligned CNT electrode [97]. The hydrophobicity of VACNTs ensures the prevention of water condensation on the cathode, resulting in long-term PEMFC stability achieved by their ability to control water balance and gas diffusion [98,99].
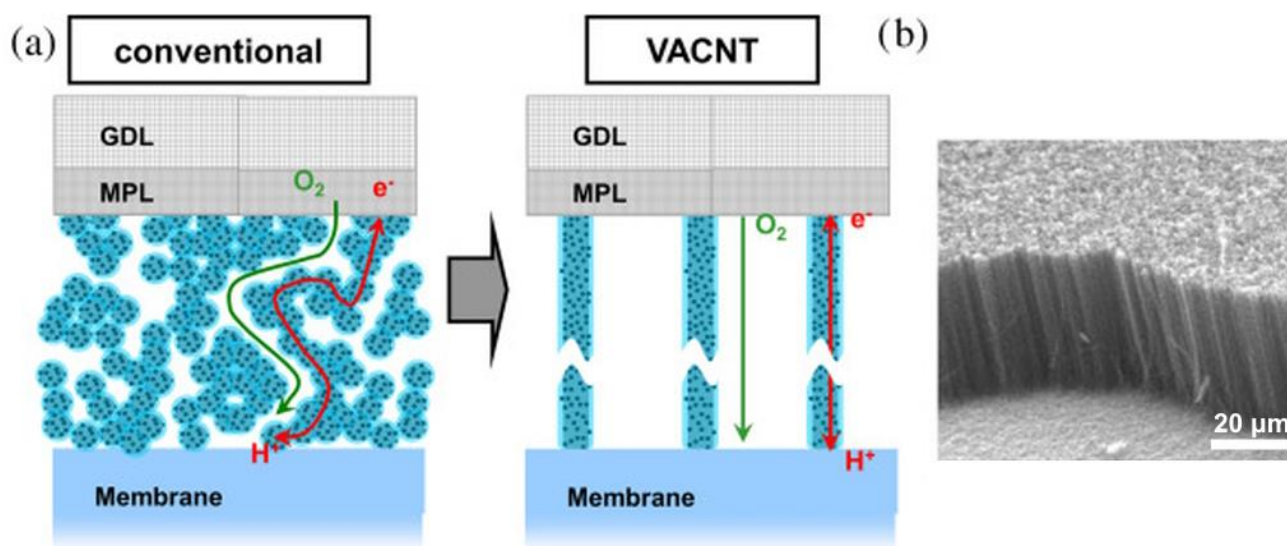

Figure 4. (**a**) Concept of VACNT electrodes; (**b**) SEM image of VACNTs [100]. Copyright 2014, Elsevier.

The formation of an electrode with MPL representing VACNTs is the most promising direction of development [100]. The concept of the electrode based on aligned nanotubes is shown in Figure 4. Here, nanotubes are grown vertically directly on the GDL, on which platinum catalytic particles are subsequently deposited. In this case, the diffusion of reagents due to the structure of the support is directed through the channels of the VACNT array with the catalyst, which enhances the chemisorption of gas reagents. The vertically aligned structure enhances the gas diffusivity, water transport, and effective utilization of Pt [100]. The platinum particle nanotube-based electrodes also provide improved proton and electron transport by creating an electrical contact between the substrate and CNTs, which greatly enhances the properties of the PEMFC device [99]. The thus-obtained carbon nanotube array is perpendicularly aligned along the entire length of the carbon fibers and covers the surface of the GDL. Fuel cell tests have demonstrated performance improvements of up to 30% [101].

The MPL structure for FC is also created by the direct growth of thin multi-walled VACNTs on a commercial GDL carbon fiber substrate without hydrophobic treatment [101].

In this case, it is possible to control the layer thickness by means of the layer-by-layer buildup of the CNT array. The formation of the near-surface catalytic layer based on MWCNTs as part of the microporous layer of the electrode is also carried out by methods that do not disturb the structure of the carbon support. When Pt-catalyst particles are attached to the top of the VACNT adjacent to the proton exchange membrane, the active region of the three-phase interface grows. Simultaneously, preserving the mass transport channels between the VACNTs without metal catalyst particles ensures the removal of reagents, which has a positive effect on the PEMFC performance [97]. It is possible to increase the three-phase interface between the catalyst, its support, and the PEM. The high peak power density of 1.61 W/cm^2 (H$_2$/O$_2$, 150 kPa) at an ultra-low Pt loading of 50 μg/cm^2 in this case is attributed to the presence of ordered hydrophobic and hydrophilic regions along the VACNTs. These regions ensure sufficient membrane wetting and promote rapid H$_3$O$^+$ transport, resulting in high Pt utilization, as well as facilitate mass transfer at high current densities [97].

Thus, CNTs, particularly vertically aligned nanotubes, are the most effective solution for addressing the issue of reagent mass transfer during MEA operation, which is due to the optimized structure of catalyst layers with mass transport channels and high adhesion to the membrane, or GDL.

4. Functionalization and Doping of Structured Materials

To enhance the adhesion between catalytic nanoparticles and the surface of the structured support and to increase the reactivity of CNTs by creating active sites that facilitate the distribution of catalyst nanoparticles, the support undergoes chemical or physical pre-modification [102–106]. In the case of chemical (or covalent) functionalization, new functional groups are attached to the carbon atoms [107]. Physical groups or atoms are attached through physical sorption [108], or surface defects are created. When functionalizing CNTs, one of the best options is to use a mixture of nitric and sulfuric acids [109]. The mechanism of action of such treatment is shown in Figure 5. This treatment is carried out to form various functional groups on the surface of nanotubes [110], such as carboxyl groups, thiol groups, etc.
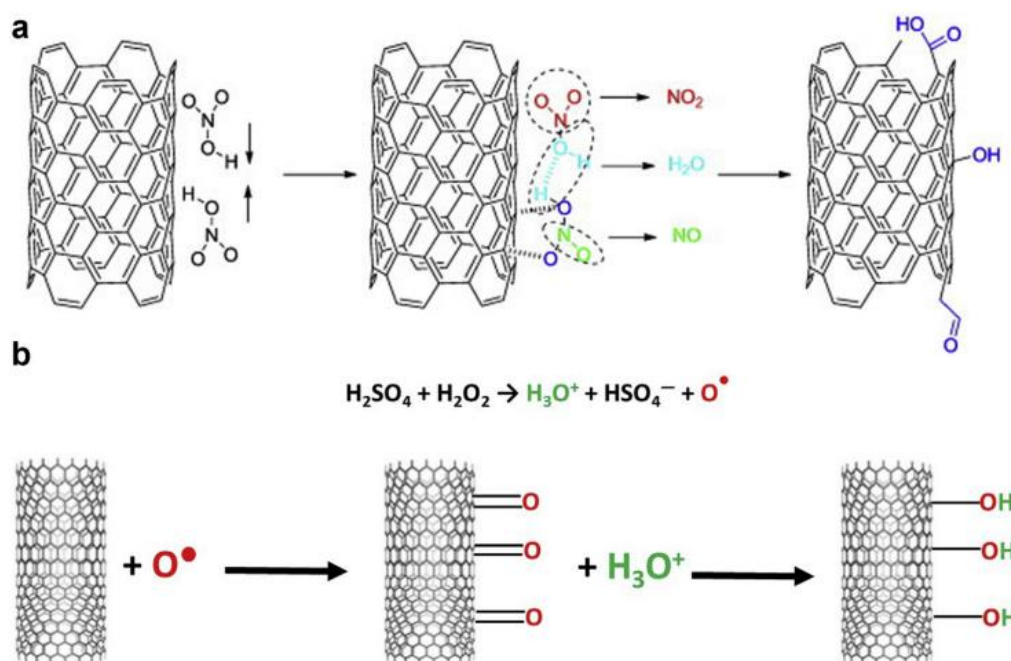

Figure 5. (**a**) Mechanism of oxidation of nitric acid; (**b**) mechanism of oxidation of piranha solution [104]. Copyright 2021, Elsevier.

In order to improve the physical and chemical properties of graphene materials, they are modified with various additives. Both heteroatoms, such as S [111], N [40,112–114], P [115,116], F [117], and various compounds, such as tin oxides [118,119], silicon oxides [120], and others [121], can serve as doping materials. These additives are introduced into the graphite structure by various chemical and physical methods and act as functional groups. Figure 6 shows the reaction schemes employed during the synthesis of modified CNTs by two distinct methods: adsorbed melamine polymerization (1) and melamine-formaldehyde resin polymerization on the CNT surface (2). As previously discussed, in catalyst support synthesis, catalytic nanoparticles are incorporated into the graphene lattice by replacing heteroatoms or attaching to functional groups that serve as adsorption sites. This enhances the interaction between the materials, resulting in better electrochemical activity and stability of the catalyst layer [112]. Also, the presence of doping components leads to an increase in the electrode–electrolyte interface, which contributes to lower resistance and improved conductivity and leads to an improvement in the overall performance of the fuel cell [115]. Heteroatom-doped graphenes and their derivatives can also exhibit catalytic properties comparable to classical Pt/C-type catalysts, which can significantly reduce the cost of FC due to the absence of expensive metals [122,123].
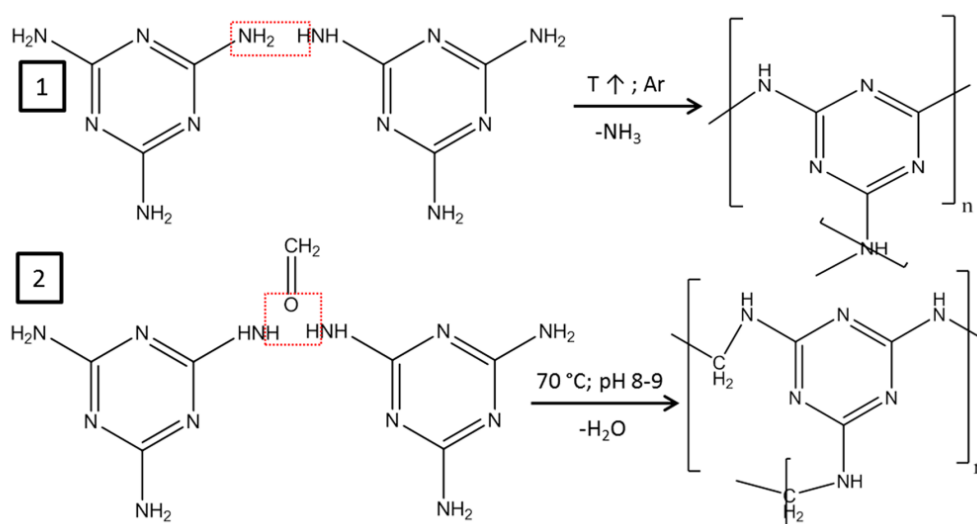

Figure 6. Synthesis scheme of nitrogen-containing polymers on the surface of CNTs. (**1**) Polymerization of melamine; (**2**) synthesis of a melamine–formaldehyde resin [83]. Copyright 2019, Springer.

CNTs, just like graphene, are doped with various heteroatoms to increase the durability of the catalytic layer. By using modifying compounds, it is possible to prevent direct contact between carbon and water, reducing the corrosion of carbon in electrochemical reactions [124]. Introducing modifying atoms directly into the carbon lattice results in increased durability and maximum power density of the PEMFC [125–127]. Modification of CNTs results in a reduction in the average size of Pt particles, which is due to an increase in the concentration of Pt ion anchoring sites during the synthesis of Pt/CNT catalysts. This, in turn, can lead to a higher utilization rate of the active component Pt observed in both the electrochemical cell and PEMFCs [50,83,124]. The effective doping also showed a reduction in excessively defective carbon atoms [78]. Nitrogen doping can increase catalytic activity, making this method attractive for ORR catalyst support [107,128,129].

5. Other Carbon Structures

5.1. Carbon Spheres

Carbon spheres are a type of carbon material that has a large surface area and a mesoporous structure [130–132]. These characteristics make them excellent for use as a support for platinum catalysts. The mesoporous structure of the carbon spheres provides

a large surface area for the distribution of Pt nanoparticles, which increases the ESA of the catalyst. The porous nature of the carbon spheres also provides better access for reagent molecules to the Pt nanoparticles, resulting in improved catalytic and transport characteristics. Furthermore, carbon spheres exhibit excellent mechanical stability and thermal conductivity, rendering them a dependable and long-lasting support material for platinum catalysts. In general, mesoporous carbon spheres are promising materials for the development of highly efficient platinum catalysts for various applications.

Various parameters of carbon spheres, including their size, structure, and the number of shells, can be customized to meet specific needs. The design and creation of functional carbon spheres have garnered significant attention in the realm of research. As the demand for materials in energy conversion continues to grow, the fabrication of carbon spheres and their derivatives has become increasingly sophisticated, moving from simple to complex structures. This process involves modifying both the outer shell and the internal architecture of the spheres. As a result, a combination of three different methods (hard, soft, and self-templating) is utilized alongside a range of preparation techniques (such as selective etching, nanocasting, chemical vapor deposition, and spray pyrolysis) to achieve the desired outcomes [133–141].

Hard templating methods involve using rigid particles as templates to create hollow structures, which are removed after the desired shells are formed. For example, in the case of single-shelled carbon spheres, a carbonaceous precursor is coated on the template and then converted into a carbon shell through a carbonization process. The template is then selectively removed to create a carbon nanomaterial with internal void space. While removing hard templates can be a time-consuming process, it allows for the production of carbon spheres with a narrow size distribution and good morphological uniformity. Various templates, like silica, polymer, and metallic spheres, can be easily fabricated for this purpose. While hard templates require laborious removal by acid/alkaline etching or organic solvent dissolution, soft templating offers a more convenient and environmentally friendly approach through the self-assembly of precursor molecules with colloidal systems as templates, easily removed by pyrolysis or extraction. The self-templating method is an efficient way to prepare hollow carbon spheres without the need for additional templates. Solid or hollow polymer spheres can be directly synthesized and converted to hollow carbon spheres through self-assembly and calcination treatment.

In general, the choice of carbon sphere synthesis method for PEMFC will depend on the desired properties of the spheres, such as size, morphology, surface area, and pore structure. Each method has its own advantages and limitations. Careful optimization of synthesis parameters is crucial to achieving the desired performance in PEMFC.

One new approach is to develop a platinum catalyst without support, in which carbon spheres are used as a framework for the deposition of platinum particles and then removed. The electrocatalyst exhibits a surface area similar to that of commercial Pt/C, as determined by electrochemical studies. Additionally, based on DST results, it demonstrates twice the durability of Pt/C [130]. When using spheres as a support, their organized porous structure provides a combination of high electrocatalytic activity in ORR and high mass transfer efficiency. A well-designed porous structure and microstructure provide an optimized water/gas transport pathway into the fuel cell CLs [131].

It is also possible to synthesize a Pt catalyst using a new carbon support, a cup-shaped hollow carbon hemisphere (and an N-doped hemisphere) (carbon shell thickness ~ 4.6 nm). This morphology allows for good bonding of the broken shells and Pt loading on both sides. In addition, carbon has pores that are sized to match the size of the Pt particles, which results in their filling with Pt, as well as clogging the pores and, as a consequence, limiting the agglomeration of Pt, as determined by in situ XRD analysis. Both catalysts show high ESA (60–65 m^2/g) and cyclic durability (6000 cycles), which is superior to the commercial Pt/C catalyst. This enhanced durability under potential cycling can also be attributed to the pore size and limitations of Pt dissolution, as well as improved metal–substrate interaction [132].

5.2. Aerogels

Aerogels are a type of ultralight, highly porous material that is promising for use in PEMFC. Aerogels have a large surface area, which can provide a larger active area for chemical reactions to take place. This can improve the efficiency of the fuel cell and increase its output power. In addition, aerogels have good thermal stability and low thermal conductivity to maintain the operating temperature of the fuel cell and improve its overall performance. Furthermore, aerogels can be easily customized to obtain specific properties, such as pore size, surface area, and surface chemical composition, which can be optimized for use in PEMFCs. The process of preparing carbon gels consists of three main steps: polymerization, dehydration, and carbonization [142–149]. During the polymerization phase, hydrogels are formed through the combination and linking of molecules. Hydroxymethyl groups are added to resorcinol, which then undergoes condensation to form methylene and methylene–ether bridges. Crosslinking and agglomeration create the 3D hydrogel structure. Various alkali and acid catalysts are used in the addition and condensation reactions. Organic carbon aerogels can be synthesized using different aromatic aldehyde pairs and templating agents for specific properties.

Recently, graphene, carbon nanotubes, and biomass have been proposed as easier-to-use alternatives to traditional polymers. Various techniques, such as sol–gel, template, spacer support, self-support, and substrate-based methods, have been employed to create graphene aerogels. CNT-derived aerogels show potential as electrically conductive materials as they link together through van der Waals forces. However, directly forming CNT-based aerogels presents challenges like weak 3D structure, mechanical fragility, and limited flexibility. To address these issues, surfactants can be added to reduce CNT surface activity, and polymer additives can be used to strengthen the network.

As shown, the mesopore volume of the electrocatalyst on carbon aerogel by Brunauer–Emmett–Teller (BET) analysis is 2.7 times larger and the ESA is 2.2 times larger compared with that of conventional carbon black. Electrochemical durability experiments show greater stability of carbon aerogel compared to carbon black [150].

Using aerogel can increase the maximum power output of the fuel cell by 10% while maintaining its high performance and lowering potential losses for a wider current range. The carbon aerogel synthesized by the sol–gel method allows the platinum content in the electrocatalyst to be reduced to 4.2 wt.%. Platinum on carbon aerogel exhibits high catalytic activity in the ORR, with an ESA of 188 m^2/g_{Pt}. The high activity of the electrocatalyst on aerogel in the ORR is determined by its large mesoporosity, uniform distribution of dispersed Pt nanoparticles, and small size. The method used to prepare this electrocatalyst can be described as classical and relatively simple, making it suitable for mass production [151].

5.3. Other Structures

Carbon nanocages, nanohorns, nanocoils, uniform porous networks, and nano-onions are all viable carbon materials for PEMFCs [152–156].

The unique cellular structure of carbon nanocages can provide a large surface area and excellent conductivity, making them ideal for maximizing PEMFC efficiency and performance. The hollow interior of the carbon nanocages can provide improved mass transfer and accessibility of platinum sites, resulting in improved catalytic activity and stability of the electrocatalyst.

Carbon nanohorns, discovered in 1998, are interesting nanomaterials due to their special morphology and physicochemical properties. The carbon nanohorn structure consists of single graphene tubes with highly stressed tapered tips that aggregate into larger spherical angular superstructures with diameters of approximately 100 nm. The carbon nanohorns possess an unconventional structure, high purity and porosity, good electrical conductivity, and a large surface area, making them a promising electrocatalyst support. Like carbon nanotubes, carbon nanohorns are also insoluble in solvents, making it difficult to handle and use them effectively. Functionalization is a useful technique to improve the solubility of carbon nanohorns by oxidizing the tips, which have the

most defects, increasing surface area and access to internal space. Covalent modification methods involve adding carboxylic groups to the tips of carbon nanohorns after oxidation or attaching organic molecules to the outer structure through cycloaddition reactions (Figure 7).
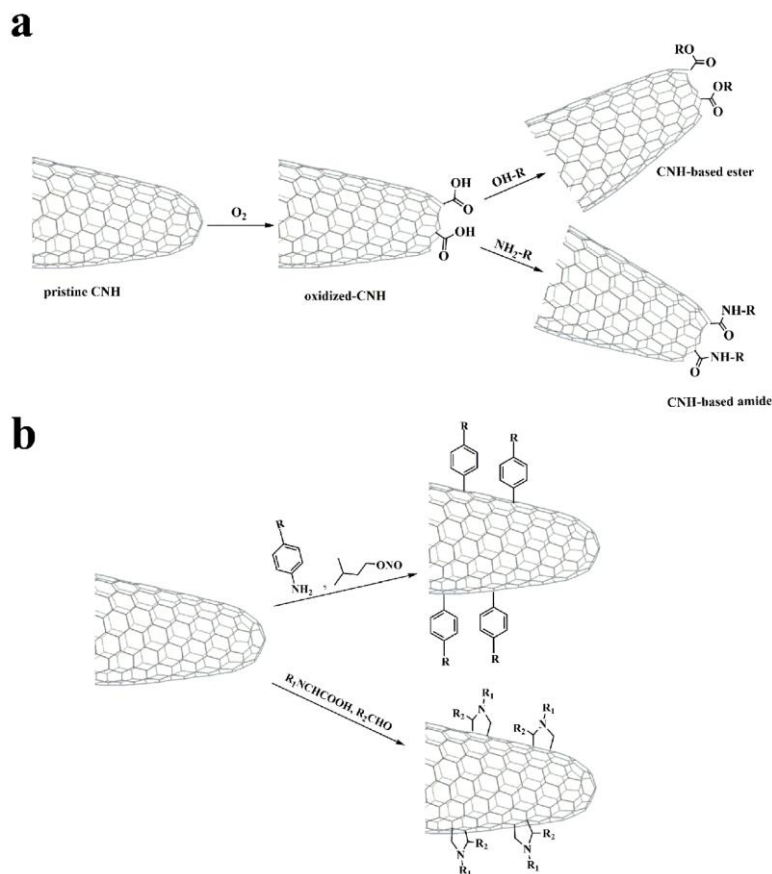

Figure 7. (**a**) Oxidation of carbon nanohorns and further post-functionalization of oxidized carbon nanohorns. (**b**) Functionalization of carbon nanohorns within situ-generated aryl diazonium salts and via the 1,3-dipolar cycloaddition reaction of in situ-generated azomethine ylides [153]. Copyright 2020, MDPI.

Carbon nanocoils are a unique form of carbon nanomaterial characterized by their distinctive helical structure, which resembles the miniature coils of a spring. They typically consist of sp^2-hybridized carbon atoms, which give them exceptional physical and chemical properties. Nanocoils have a large surface area, excellent electrical and thermal conductivity, and mechanical flexibility due to their helical morphology. These properties make them promising candidates for a variety of applications, including nanoelectronics, sensors, energy storage, and catalysis. In the context of energy applications, nanocoils have been studied for their potential use in fuel cells, supercapacitors, and batteries. Their large surface area and electrical conductivity could improve performance and efficiency [157,158].

Ordered homogeneous porous carbon networks are three-dimensional carbon structures with a well-defined and regular porous morphology. These networks have a large surface area, a uniform distribution of pore sizes, and interconnected porosity, making them ideal for various applications, such as energy storage, catalysis, and gas separation. The ordered and homogeneous nature of carbon networks provides improved mass transfer and reaction kinetics [159,160].

Carbon nano-onions are a unique form of carbon nanoparticles consisting of concentric graphite layers similar to those of an onion. They are formed by arc discharge, in which layers of graphene are forced to form spherical onion-like structures. Due to the unique structure of carbon nano-onions, they have outstanding properties such as high mechanical

strength, excellent thermal and electrical conductivity, and a large surface area. These properties make them suitable for a variety of applications, including energy storage, nanocomposites, and biomedical applications.

The study of various nanostructured carbon materials is crucial for developing new types of electrodes that can enhance the performance, durability, and applicability of fuel cell technology. However, it is important to consider the economics and complexity of methods for synthesizing and scaling production of such carbon structures to improve the economic viability of fuel cell technology.

6. Summary and Conclusions

This review highlights the recent success of the use of carbon-based structures as electrodes, including PEMFC electrochemical performance. The use of structured supports shows promise in improving the efficiency and durability of electrodes for PEMFCs. Structured carbon materials, such as graphene, its oxides, and derivatives, including CNTs and their arrays, are the most promising for use in PEMFCs as electrocatalyst supports and additives in CL and GDL due to their well-developed surface and high degradation stability. Catalysts, on the other hand, exhibit improved electrocatalytic activity, stability, and degradation resistance due to the interaction between the support and active metal particles. This is achieved through the partial incorporation of platinum into the carbon material structure, resulting in increased dispersion of platinum particles during synthesis. However, the operation of MEAs with CL/GDL formed on the basis of structured carbon materials involves mass and gas transfer problems, which negatively affect the overall FC performance. The successful application of electrocatalytic material as a component of the PEMFC layer depends on its effectiveness as a support for the electrocatalyst, which must provide high values of electrical conductivity, dispersibility, and ESA of deposited particles, as well as their stability. Additionally, the ability to create a porous structure with sufficient values of mass transfer, reagent inlet/outlet characteristics, and hydrophilic/hydrophobic properties is essential.

Table 1 presents a summary of data from the recent literature that characterizes the main attributes of CLs based on structured graphene materials, as well as the performance of the PEMFC based on them. However, a deeper analysis of the literature reveals that there is insufficient data on the performance of PEMFCs due to the existing problems of reagent mass transfer. Thus, specific research aimed at improving the architecture of such electrodes to increase their specific capacity by improving mass transport makes this topic relevant [161].

It is important to note that, despite the similarity of the properties of the considered structures, the differences in their architecture and composition of surface groups and defects become determinative with regard to their application as electrode materials for PEMFC. Graphenes and their derivatives appear to be the most promising candidates for use as electrocatalyst support, but difficulties with the formation of an effective graphene-based layer have led to an almost complete absence of their testing in PEMFC, making the research of catalysts based on them a dead end. CNTs, in particular their arrays, appear to have greater potential. It is possible to form a catalytic layer of effective architecture with high diffusion characteristics, sufficient water balance, and improved power characteristics of the device. This issue is partially solved for vertically aligned carbon nanotubes due to their optimized structure, strong adhesion to GDL, and the existence of mass transport channels. The functionalization of this support and improvement of the properties of catalysts based on it may lead to even more successful results in terms of PEMFC technology. However, the task of optimizing the structure and porosity of graphene-like materials to enhance PEMFC efficiency remains relevant.

Table 1. A summary of data from the recent literature that characterizes the main attributes of CLs based on structured graphene materials, as well as the performance of the PEMFC based on them.

		Graphene Structures		Carbon Nanotubes		Other Structures
	Advantages	High dispersion of deposited platinum, ESA value, stability, and durability of catalysts. Increasing FC output power when used as an additive		High catalyst stability and durability Ultra-low platinum loading High power output (both as a catalyst and as an electrode additive)		High dispersion of deposited platinum, ESA value, stability, and durability of catalysts Ultra-low platinum loading
	Disadvantages	Low values of mass transfer and diffusion of reagents in the layer Not applicable as a catalytic layer		Low dispersion of deposited platinum and ESA value of the catalysts		Complex fabrication technology Low FC output power No data
	Issue	Formation of the catalytic layer architecture		Functionalization to increase the dispersion of the active metal		Expanding research
	Parameters	Graphene nanosheets	Graphene oxides and reduced graphene oxides	Carbon nanotubes	Vertically aligned CNTs	**Other structures**
Electrocatalyst	ESA, m^2/g	80–100 [48,50]	20–50 [41,64,66]	10–40 [75,85,88]	~30 [98]	~200 [132,150]
Electrocatalyst	Degradation (ESA losses), %	~5	10–30	~30	~5	~35
Electrocatalyst	Composition	40 wt. % Pt/G	16.9 wt. % Pt/T-RGO	10 wt. % Pt/CNT	Pt-Co/VACNTs	40 wt. % Pt/broken hollow C spheres, 30 wt. % Pt/aerogels
Catalytic layer	CL architecture	-	40 wt. % Pt/rGO	Nafion ionomer, isopropanol, and 0.125 mg/cm^2 mMWCNT	Pt/VACNTs on cathode, VACNTs were used as MPL with a thickness of 4.6 μm	30 wt. % Pt/aerogels
Catalytic layer	Pt loading on anode/cathode, mg/cm^2	-	0.2/0.2 Pt/rGO on cathode Pt/C on anode	0.06/0.06 Pt/C (cathode) and PtRu/C (anode)	0.2/0.2	0.1/0.1
Catalytic layer	Maximum power density, W/cm^2	-	~0.62 [62]	~1.2 [91]	~1.4 [97]	~0.33 [150]
Electrode	Electrode architecture	Double-layer GDL with graphene MPL; MPL thickness 13–17 μm; mean pore size 162.41 nm	rGO was a capacitive material; pore diameter between 0.7 and 9 μm; a 60 wt. % Pt/C catalyst was applied to the GDL on top	Normal carbon black GDL without MPL and with 15 μm thick CNT sheet MPLs	VACNTs were used as MPLs with a thickness of ~40 μm; total porosity 56.3%	-
Electrode	Maximum power density, W/cm^2	~0.95 [48]	~0.75 [64]	~0.74 [89]	~1.41 [98]	-

In the field of other carbon structures, the question of the optimal balance between the increasing complexity of material fabrication technology and the success and reproducibility of the results obtained remains open. When using complex carbon nanostructures, such as spheres, it is crucial to evaluate the technological and economic efforts required against the benefits they provide in terms of catalyst properties and device performance.

Conflicts of Interest: The authors declare no conflicts of interest.

References

1. Mensharapov, R.M.; Ivanova, N.A.; Spasov, D.D.; Kukueva, E.V.; Zasypkina, A.A.; Seregina, E.A.; Grigoriev, S.A.; Fateev, V.N. Carbon-Supported Pt-SnO₂ Catalysts for Oxygen Reduction Reaction over a Wide Temperature Range: Rotating Disk Electrode Study. *Catalysts* **2021**, *11*, 1469. [CrossRef]

2. Zhao, H.; Xing, T.; Li, L.; Geng, X.; Guo, K.; Sun, C.; Zhou, W.; Yang, H.; Song, R.; An, B. Synthesis of Cobalt and Nitrogen Co-Doped Carbon Nanotubes and Its ORR Activity as the Catalyst Used in Hydrogen Fuel Cells. *Int. J. Hydrogen Energy* **2019**, *44*, 25180–25187. [CrossRef]

3. Stühmeier, B.M.; Pietsch, M.R.; Schwämmlein, J.N.; Gasteiger, H.A. Pressure and Temperature Dependence of the Hydrogen Oxidation and Evolution Reaction Kinetics on Pt Electrocatalysts via PEMFC-Based Hydrogen-Pump Measurements. *J. Electrochem. Soc.* **2021**, *168*, 064516. [CrossRef]

4. Harzer, G.S.; Orfanidi, A.; El-Sayed, H.; Madkikar, P.; Gasteiger, H.A. Tailoring Catalyst Morphology towards High Performance for Low Pt Loaded PEMFC Cathodes. *J. Electrochem. Soc.* **2018**, *165*, F770–F779. [CrossRef]

5. Mensharapov, R.M.; Spasov, D.D.; Ivanova, N.A.; Zasypkina, A.A.; Smirnov, S.A.; Grigoriev, S.A. Screening of Carbon-Supported Platinum Electrocatalysts Using Frumkin Adsorption Isotherms. *Inorganics* **2023**, *11*, 103. [CrossRef]

6. Spasov, D.D.; Ivanova, N.A.; Pushkarev, A.S.; Pushkareva, I.V.; Presnyakova, N.N.; Chumakov, R.G.; Presnyakov, M.Y.; Grigoriev, S.A.; Fateev, V.N. On the Influence of Composition and Structure of Carbon-Supported Pt-SnO2 Hetero-Clusters onto Their Electrocatalytic Activity and Durability in PEMFC. *Catalysts* **2019**, *9*, 803. [CrossRef]

7. Spasov, D.D.; Ivanova, N.A.; Mensharapov, R.M.; Zasypkina, A.A.; Seregina, E.A.; Grigoriev, S.A.; Fateev, V.N. Nanostructured Pt20/SiO₂ˣ/C Electrocatalysts for Water-Balance Stabilization in a Proton Exchange Membrane Fuel Cell. *Nanotechnologies Russ.* **2022**, *17*, 320–327. [CrossRef]

8. Ivanova, N.A.; Alekseeva, O.K.; Fateev, V.N.; Shapir, B.L.; Spasov, D.D.; Nikitin, S.M.; Presnyakov, M.Y.; Kolobylina, N.N.; Soloviev, M.A.; Mikhalev, A.I. Activity and Durability of Electrocatalytic Layers with Low Platinum Loading Prepared by Magnetron Sputtering onto Gas Diffusion Electrodes. *Int. J. Hydrogen Energy* **2019**, *44*, 29529–29536. [CrossRef]

9. Fedotov, A.A.; Grigoriev, S.A.; Millet, P.; Fateev, V.N. Plasma-Assisted Pt and Pt–Pd Nano-Particles Deposition on Carbon Carriers for Application in PEM Electrochemical Cells. *Int. J. Hydrogen Energy* **2013**, *38*, 8568–8574. [CrossRef]

10. Cai, Y.; Wu, D.; Sun, J.; Chen, B. The Effect of Cathode Channel Blockages on the Enhanced Mass Transfer and Performance of PEMFC. *Energy* **2021**, *222*, 119951. [CrossRef]

11. Jiao, D.; Jiao, K.; Zhong, S.; Du, Q. Investigations on Heat and Mass Transfer in Gas Diffusion Layers of PEMFC with a Gas–Liquid-Solid Coupled Model. *Appl. Energy* **2022**, *316*, 118996. [CrossRef]

12. Jeng, K.T.; Lee, S.F.; Tsai, G.F.; Wang, C.H. Oxygen Mass Transfer in PEM Fuel Cell Gas Diffusion Layers. *J. Power Sources* **2004**, *138*, 41–50. [CrossRef]

13. Mensharapov, R.; Ivanova, N.; Spasov, D.; Grigoriev, S.; Fateev, V. SAXS Investigation of the Effect of Freeze/Thaw Cycles on the Nanostructure of Nafion® Membranes. *Polymers* **2022**, *14*, 4395. [CrossRef] [PubMed]

14. Ivanova, N.A.; Spasov, D.D.; Grigoriev, S.A.; Kamyshinsky, R.A.; Peters, G.S.; Mensharapov, R.M.; Seregina, E.A.; Millet, P.; Fateev, V.N. On the Influence of Methanol Addition on the Performances of PEM Fuel Cells Operated at Subzero Temperatures. *Int. J. Hydrogen Energy* **2021**, *46*, 18116–18127. [CrossRef]

15. Rodgers, M.P.; Bonville, L.J.; Kunz, H.R.; Slattery, D.K.; Fenton, J.M. Fuel Cell Perfluorinated Sulfonic Acid Membrane Degradation Correlating Accelerated Stress Testing and Lifetime. *Chem. Rev.* **2012**, *112*, 6075–6103. [CrossRef] [PubMed]

16. Ren, P.; Pei, P.; Li, Y.; Wu, Z.; Chen, D.; Huang, S. Degradation Mechanisms of Proton Exchange Membrane Fuel Cell under Typical Automotive Operating Conditions. *Prog. Energy Combust. Sci.* **2020**, *80*, 100859. [CrossRef]

17. Jahnke, T.; Futter, G.; Latz, A.; Malkow, T.; Papakonstantinou, G.; Tsotridis, G.; Schott, P.; Gérard, M.; Quinaud, M.; Quiroga, M.; et al. Performance and Degradation of Proton Exchange Membrane Fuel Cells: State of the Art in Modeling from Atomistic to System Scale. *J. Power Sources* **2016**, *304*, 207–233. [CrossRef]

18. Kregar, A.; Kravos, A.; Katrašnik, T. Methodology for Evaluation of Contributions of Ostwald Ripening and Particle Agglomeration to Growth of Catalyst Particles in PEM Fuel Cells. *Fuel Cells* **2020**, *20*, 487–498. [CrossRef]

19. Fan, L.; Zhao, J.; Luo, X.; Tu, Z. Comparison of the Performance and Degradation Mechanism of PEMFC with Pt/C and Pt Black Catalyst. *Int. J. Hydrogen Energy* **2022**, *47*, 5418–5428. [CrossRef]

20. Urchaga, P.; Kadyk, T.; Rinaldo, S.G.; Pistono, A.O.; Hu, J.; Lee, W.; Richards, C.; Eikerling, M.H.; Rice, C.A. Catalyst Degradation in Fuel Cell Electrodes: Accelerated Stress Tests and Model-Based Analysis. *Electrochim. Acta* **2015**, *176*, 1500–1510. [CrossRef]

21. Li, C.; Zhu, L.; Song, L.; Zhu, G.; Zhang, Q.; Zhao, Y.; Gong, Q.; Sun, C.; Liu, Y.; Sasaki, K.; et al. Synergistic effect of polyaniline on stabilizing Pt nanoparticles in PEMFCs. *J. Mater. Chem. A* **2023**, *11*, 7756–7766. [CrossRef]

22. Meier, J.C.; Galeano, C.; Katsounaros, I.; Witte, J.; Bongard, H.J.; Topalov, A.A.; Baldizzone, C.; Mezzavilla, S.; Schüth, F.; Mayrhofer, K.J.J. Design Criteria for Stable Pt/C Fuel Cell Catalysts. *Beilstein J. Nanotechnol.* **2014**, *5*, 44–67. [CrossRef] [PubMed]

23. Liu, F.; Gao, Z.; Su, J.; Guo, L. An Experimental Investigation of the Effect of Platinum on the Corrosion of Cathode Carbon Support in a PEMFC. *ChemSusChem* **2022**, *12*, e202102726. [CrossRef] [PubMed]

24. Liu, P.; Yang, D.; Li, B.; Qu, T.; Ming, P.; Zhang, C.; Pan, X. Agglomeration behavior of carbon-supported platinum nanoparticles in catalyst ink: Modeling and experimental investigation. *J. Power Sources* **2024**, *602*, 234309. [CrossRef]

25. Ettingshausen, F.; Kleemann, J.; Marcu, A.; Toth, G.; Fuess, H.; Roth, C. Dissolution and Migration of Platinum in PEMFCs Investigated for Start/Stop Cycling and High Potential Degradation. *Fuel Cells* **2011**, *11*, 238–245. [CrossRef]

26. Pushkarev, A.S.; Pushkareva, I.V.; Ivanova, N.A.; du Preez, S.P.; Bessarabov, D.; Chumakov, R.G.; Stankevich, V.G.; Fateev, V.N.; Evdokimov, A.A.; Grigoriev, S.A. Pt/C and Pt/SnOx/C Catalysts for Ethanol Electrooxidation: Rotating Disk Electrode Study. *Catalysts* **2019**, *9*, 271. [CrossRef]

27. Das, B.; Das, S.; Tewary, S.; Bose, S.; Ghosh, S.; Ghosh, A. Graphene Nano Sheets for the Fuel Cell Applications. In *Advances in Nanosheets [Working Title]*; IntechOpen: London, UK, 2023.

28. Voznyakovskii, A.; Vozniakovskii, A.; Kidalov, S. New Way of Synthesis of Few-Layer Graphene Nanosheets by the Self Propagating High-Temperature Synthesis Method from Biopolymers. *Nanomaterials* **2022**, *12*, 657. [CrossRef] [PubMed]

29. Kozlova, M.; Butrim, S.; Solovyev, M.; Pushkarev, A.; Pushkareva, I.; Kalinichenko, V.; Akelkina, S.; Grigoriev, S. Structural and Electrochemical Characteristics of Platinum Nanoparticles Supported on Various Carbon Carriers. *C* **2022**, *8*, 14. [CrossRef]

30. Wang, K.; Zhou, T.; Cao, Z.; Yuan, Z.; He, H.; Fan, M.; Jiang, Z. Advanced 3D Ordered Electrodes for PEMFC Applications: From Structural Features and Fabrication Methods to the Controllable Design of Catalyst Layers. *Green Energy Environ.* **2023**, *in press*. S2468025723001462. [CrossRef]

31. Zasypkina, A.A.; Ivanova, N.A.; Spasov, D.D.; Mensharapov, R.M.; Alekseeva, O.K.; Vorobyeva, E.A.; Kukueva, E.V.; Fateev, V.N. Electrode with a Carbon Nanotube Array for a Proton Exchange Membrane Fuel Cell. *Inorganics* **2023**, *11*, 219. [CrossRef]

32. Verma, V.; Choudhury, S.R.; Rathour, V.; Choudhury, S.R.; Ganesan, V. Hollow Core Mesoporous Carbon Spheres as Catalyst Support for Improved Platinum Utilization in Phosphoric Acid Fuel Cells. *Microporous Mesoporous Mater.* **2024**, *367*, 113005. [CrossRef]

33. Mamat, M.S.; Grigoriev, S.A.; Dzhus, K.A.; Grant, D.M.; Walker, G.S. The Performance and Degradation of Pt Electrocatalysts on Novel Carbon Carriers for PEMFC Applications. *Int. J. Hydrogen Energy* **2010**, *35*, 7580–7587. [CrossRef]

34. Luo, C.; Xie, H.; Wang, Q.; Luo, G.; Liu, C. A Review of the Application and Performance of Carbon Nanotubes in Fuel Cells. *J. Nanomater.* **2015**, *2015*, 560392. [CrossRef]

35. Ortiz-Herrera, J.C.; Cruz-Martínez, H.; Solorza-Feria, O.; Medina, D.I. Recent Progress in Carbon Nanotubes Support Materials for Pt-Based Cathode Catalysts in PEM Fuel Cells. *Int. J. Hydrogen Energy* **2022**, *47*, 30213–30224. [CrossRef]

36. Su, H.; Hu, Y.H. Recent Advances in Graphene-based Materials for Fuel Cell Applications. *Energy Sci. Eng.* **2021**, *9*, 958–983. [CrossRef]

37. Sharma, S.; Pollet, B.G. Support Materials for PEMFC and DMFC Electrocatalysts—A Review. *J. Power Sources* **2012**, *208*, 96–119. [CrossRef]

38. Shaari, N.; Kamarudin, S.K. Graphene in Electrocatalyst and Proton Conductiong Membrane in Fuel Cell Applications: An Overview. *Renew. Sustain. Energy Rev.* **2017**, *69*, 862–870. [CrossRef]

39. Pushkareva, I.V.; Pushkarev, A.S.; Kalinichenko, V.N.; Chumakov, R.G.; Soloviev, M.A.; Liang, Y.; Millet, P.; Grigoriev, S.A. Reduced Graphene Oxide-Supported Pt-Based Catalysts for PEM Fuel Cells with Enhanced Activity and Stability. *Catalysts* **2021**, *11*, 256. [CrossRef]

40. Öztürk, A.; Bayrakçeken Yurtcan, A. Raw and Pyrolyzed (with and without Melamine) Graphene Nanoplatelets with Different Surface Areas as PEM Fuel Cell Catalyst Supports. *Carbon Lett.* **2021**, *31*, 1191–1214. [CrossRef]

41. Lagarteira, T.; Delgado, S.; Fernandes, C.; Azenha, C.; Mateos-Pedrero, C.; Mendes, A. The Role of Pt Loading on Reduced Graphene Oxide Support in the Polyol Synthesis of Catalysts for Oxygen Reduction Reaction. *Int. J. Hydrogen Energy* **2020**, *45*, 20594–20604. [CrossRef]

42. Smirnov, S.A.; Mensharapov, R.M.; Spasov, D.D.; Ivanova, N.A.; Grigoriev, S.A. Adsorption and Recombination of H+ and H3O+ on Graphene-Supported Pt1, Pt13, and Pt14 Nanoclusters: A First Principles Study. *Catalysts* **2024**, *14*, 108. [CrossRef]

43. Choi, S.M.; Seo, M.H.; Kim, H.J.; Kim, W.B. Synthesis of Surface-Functionalized Graphene Nanosheets with High Pt-Loadings and Their Applications to Methanol Electrooxidation. *Carbon* **2011**, *49*, 904–909. [CrossRef]

44. Tran, T.; Song, M.Y.; Kang, T.; Samdani, J.; Park, H.; Kim, H.; Jhung, S.H.; Yu, J. Iron Phosphide Incorporated into Iron-Treated Heteroatoms-Doped Porous Bio-Carbon as Efficient Electrocatalyst for the Oxygen Reduction Reaction. *ChemElectroChem* **2018**, *5*, 1944–1953. [CrossRef]

45. Lee, F.C.; Ismail, M.S.; Zhang, K.; Ingham, D.B.; Aldakheel, F.; Hughes, K.J.; Ma, L.; El-Kharouf, A.; Pourkashanian, M. Optimisation and Characterisation of Graphene-Based Microporous Layers for Polymer Electrolyte Membrane Fuel Cells. *Int. J. Hydrogen Energy* **2024**, *51*, 1311–1325. [CrossRef]

46. Chen, J.; Bailey, J.J.; Britnell, L.; Perez-Page, M.; Sahoo, M.; Zhang, Z.; Strudwick, A.; Hack, J.; Guo, Z.; Ji, Z.; et al. The Performance and Durability of High-Temperature Proton Exchange Membrane Fuel Cells Enhanced by Single-Layer Graphene. *Nano Energy* **2022**, *93*, 106829. [CrossRef]

47. Tanuma, T.; Kawamoto, M.; Kinoshita, S. Effect of Properties of Hydrophilic Microporous Layer (MPL) on PEFC Performance. *J. Electrochem. Soc.* **2017**, *164*, F499–F503. [CrossRef]

48. Ozden, A.; Shahgaldi, S.; Zhao, J.; Li, X.; Hamdullahpur, F. Assessment of Graphene as an Alternative Microporous Layer Material for Proton Exchange Membrane Fuel Cells. *Fuel* **2018**, *215*, 726–734. [CrossRef]

49. Fang, X.-Y.; Yu, X.-X.; Zheng, H.-M.; Jin, H.-B.; Wang, L.; Cao, M.-S. Temperature- and Thickness-Dependent Electrical Conductivity of Few-Layer Graphene and Graphene Nanosheets. *Phys. Lett. A* **2015**, *379*, 2245–2251. [CrossRef]

50. Lagarteira, T.; Delgado, S.; Garcia, G.P.; Ortiz, A.; Mendes, A. Oxygen Reduction Stability of Graphene-Supported Electrocatalyst: Electrochemical and Morphological Evidences. *Int. J. Hydrogen Energy* **2023**, *48*, 20901–20913. [CrossRef]

51. Daş, E.; Alkan Gürsel, S.; Bayrakçeken Yurtcan, A. Pt-Alloy Decorated Graphene as an Efficient Electrocatalyst for PEM Fuel Cell Reactions. *J. Supercrit. Fluids* **2020**, *165*, 104962. [CrossRef]

52. Liu, Y.; Li, Z.; Xu, S.; Xie, Y.; Ye, Y.; Zou, X.; Lin, S. Synthesis of Pt-Ni (Trace)/GNs Composite and Its Bi-Functional Electrocatalytic Properties for MOR and ORR. *J. Colloid Interface Sci.* **2019**, *554*, 640–649. [CrossRef] [PubMed]

53. Huo, L.; Liu, B.; Zhang, G.; Si, R.; Liu, J.; Zhang, J. 2D Layered Non-Precious Metal Mesoporous Electrocatalysts for Enhanced Oxygen Reduction Reaction. *J. Mater. Chem. A* **2017**, *5*, 4868–4878. [CrossRef]

54. Daş, E.; Gürsel, S.A.; Yurtcan, A.B. Simultaneously Deposited Pt-Alloy Nanoparticles over Graphene Nanoplatelets via Supercritical Carbon Dioxide Deposition for PEM Fuel Cells. *J. Alloys Compd.* **2021**, *874*, 159919. [CrossRef]

55. Boyaci San, F.G.; Dursun, S.; Yazici, M.S. PTCO on Continuous-phase Graphene as PEM Fuel Cell Catalyst. *Int. J. Energy Res.* **2021**, *45*, 1673–1684. [CrossRef]

56. Dursun, S.; Akay, R.G.; Yazici, M.S. CVD Graphene Supported Cobalt (II) Phthalocyanine as Cathode Electrocatalyst for PEM Fuel Cells. *Int. J. Hydrogen Energy* **2020**, *45*, 34837–34844. [CrossRef]

57. Chen, D.; Feng, H.; Li, J. Graphene Oxide: Preparation, Functionalization, and Electrochemical Applications. *Chem. Rev.* **2012**, *112*, 6027–6053. [CrossRef]

58. Hummers, W.S.; Offeman, R.E. Preparation of Graphitic Oxide. *J. Am. Chem. Soc.* **1958**, *80*, 1339. [CrossRef]

59. Marcano, D.C.; Kosynkin, D.V.; Berlin, J.M.; Sinitskii, A.; Sun, Z.; Slesarev, A.; Alemany, L.B.; Lu, W.; Tour, J.M. Improved Synthesis of Graphene Oxide. *ACS Nano* **2010**, *4*, 4806–4814. [CrossRef] [PubMed]

60. Grigoriev, S.A.; Fateev, V.N.; Pushkarev, A.S.; Pushkareva, I.V.; Ivanova, N.A.; Kalinichenko, V.N.; Yu Presnyakov, M.; Wei, X. Reduced Graphene Oxide and Its Modifications as Catalyst Supports and Catalyst Layer Modifiers for PEMFC. *Materials* **2018**, *11*, 1405. [CrossRef]

61. Oubraham, A.; Ion-Ebrasu, D.; Vasut, F.; Soare, A.; Sorlei, I.-S.; Marinoiu, A. Platinum-Functionalized Graphene Oxide: One-Pot Synthesis and Application as an Electrocatalyst. *Materials* **2023**, *16*, 1897. [CrossRef]

62. Marinoiu, A.; Carcadea, E.; Sacca, A.; Carbone, A.; Sisu, C.; Dogaru, A.; Raceanu, M.; Varlam, M. One-Step Synthesis of Graphene Supported Platinum Nanoparticles as Electrocatalyst for PEM Fuel Cells. *Int. J. Hydrogen Energy* **2021**, *46*, 12242–12253. [CrossRef]

63. Lazar, O.-A.; Marinoiu, A.; Raceanu, M.; Pantazi, A.; Mihai, G.; Varlam, M.; Enachescu, M. Reduced Graphene Oxide Decorated with Dispersed Gold Nanoparticles: Preparation, Characterization and Electrochemical Evaluation for Oxygen Reduction Reaction. *Energies* **2020**, *13*, 4307. [CrossRef]

64. Fu, X.; Wang, J.; Peng, F.; Wang, Y.; Hu, S.; Zhang, R.; Liu, Q. A Hybrid PEMFC/Supercapacitor Device with High Energy and Power Densities Based on Reduced Graphene Oxide/Nafion/Pt Electrode. *Int. J. Hydrogen Energy* **2023**, *48*, 16072–16082. [CrossRef]

65. Moradizadeh, L.; Yazdanpanah, P.; Karimi, G.; Paydar, M.H. Investigating the Role of Graphite and Reduced Graphene Oxide in the Fabrication of Microporous Layers for Proton Exchange Membrane Fuel Cells. *J. Mater. Sci.* **2023**, *58*, 12706–12723. [CrossRef]

66. Samancı, M.; Bayrakçeken Yurtcan, A. Chemically and Thermally Reduced Graphene Oxide Supported Pt Catalysts Prepared by Supercritical Deposition. *Int. J. Hydrogen Energy* **2022**, *47*, 19669–19689. [CrossRef]

67. Romero, A.; Lavin-Lopez, M.P.; Sanchez-Silva, L.; Valverde, J.L.; Paton-Carrero, A. Comparative Study of Different Scalable Routes to Synthesize Graphene Oxide and Reduced Graphene Oxide. *Mater. Chem. Phys.* **2018**, *203*, 284–292. [CrossRef]

68. Gomes, W.D.S.; Noce, R.D.; De Matos, T.D.S.; Andrade, F.V.; De Molfetta, F.A.; Iúdice De Souza, J.P. Cu@PtRu Core-Shell Nanostructured Electrocatalysts Anchored on Reduced Graphene Oxide Towards Methanol Oxidation. *Chem. Mater. Sci.* **2023**, *16*, 6508. [CrossRef]

69. Işıkel Şanlı, L.; Bayram, V.; Ghobadi, S.; Düzen, N.; Alkan Gürsel, S. Engineered Catalyst Layer Design with Graphene-Carbon Black Hybrid Supports for Enhanced Platinum Utilization in PEM Fuel Cell. *Int. J. Hydrogen Energy* **2017**, *42*, 1085–1092. [CrossRef]

70. Danafar, F.; Fakhru'l-Razi, A.; Salleh, M.A.M.; Biak, D.R.A. Fluidized Bed Catalytic Chemical Vapor Deposition Synthesis of Carbon Nanotubes—A Review. *Chem. Eng. J.* **2009**, *155*, 37–48. [CrossRef]

71. Esteves, L.M.; Oliveira, H.A.; Passos, F.B. Carbon Nanotubes as Catalyst Support in Chemical Vapor Deposition Reaction: A Review. *J. Ind. Eng. Chem.* **2018**, *65*, 1–12. [CrossRef]

72. Nezhad, E.Z.; Qu, X.; Musharavati, F.; Jaber, F.; Appleford, M.R.; Bae, S.; Uzun, K.; Struthers, M.; Chowdhury, M.E.H.; Khandakar, A. Effects of titanium and carbon nanotubes on nano/micromechanical properties of HA/TNT/CNT nanocomposites. *Appl. Surf. Sci.* **2021**, *538*, 148123. [CrossRef]

73. Devrim, Y.; Arıca, E.D. Multi-Walled Carbon Nanotubes Decorated by Platinum Catalyst for High Temperature PEM Fuel Cell. *Int. J. Hydrogen Energy* **2019**, *44*, 18951–18966. [CrossRef]

74. Pajootan, E.; Omanovic, S.; Coulombe, S. Controllable Dry Synthesis of Binder-Free Nanostructured Platinum Electrocatalysts Supported on Multi-Walled Carbon Nanotubes and Their Performance in the Oxygen Reduction Reaction. *Chem. Eng. J.* **2021**, *426*, 131706. [CrossRef]

75. Kim, T.; Kwon, Y.; Kwon, S.; Seo, J.G. Substrate Effect of Platinum-Decorated Carbon on Enhanced Hydrogen Oxidation in PEMFC. *ACS Omega* **2020**, *5*, 26902–26907. [CrossRef] [PubMed]
76. Aruna, I.; Mehta, B.R.; Malhotra, L.K.; Shivaprasad, S.M. Size Dependence of Core and Valence Binding Energies in Pd Nanoparticles: Interplay of Quantum Confinement and Coordination Reduction. *J. Appl. Phys.* **2008**, *104*, 064308. [CrossRef]
77. Uddin, A.S.M.I.; Yaqoob, U.; Hassan, K.; Chung, G.-S. Effects of Pt Shell Thickness on Self-Assembly Monolayer Pd@Pt Core-Shell Nanocrystals Based Hydrogen Sensing. *Int. J. Hydrogen Energy* **2016**, *41*, 15399–15410. [CrossRef]
78. Marbaniang, P.; Ingavale, S.; Karuppanan, P.; Swami, A.; Kakade, B. Rationale Approach of Nitrogen Doping at Defect Sites of Multiwalled Carbon Nanotubes: A Strategy for Oxygen Reduction Electrocatalysis. *Int. J. Hydrogen Energy* **2021**, *46*, 10268–10280. [CrossRef]
79. Devrim, Y.; Arıca, E.D. Investigation of the Effect of Graphitized Carbon Nanotube Catalyst Support for High Temperature PEM Fuel Cells. *Int. J. Hydrogen Energy* **2020**, *45*, 3609–3617. [CrossRef]
80. Li, B.; Wang, J.; Yuan, Y.; Ariga, H.; Takakusagi, S.; Asakura, K. Carbon Nanotube-Supported RuFe Bimetallic Nanoparticles as Efficient and Robust Catalysts for Aqueous-Phase Selective Hydrogenolysis of Glycerol to Glycols. *ACS Catal.* **2011**, *1*, 1521–1528. [CrossRef]
81. Haque, M.A.; Sulong, A.B.; Majlan, E.H.; Loh, K.S.; Husaini, T.; Rosli, R. Oxygen reduction reaction behaviours of carbon nanotubes supporting pt catalyst for proton exchange membrane fuel cell. *MJAS* **2019**, *23*, 147–154. [CrossRef]
82. Ivanova, N.A.; Spasov, D.D.; Zasypkina, A.A.; Alekseeva, O.K.; Kukueva, E.V.; Vorobyeva, E.A.; Kudinova, E.S.; Chumakov, R.G.; Millet, P.; Grigoriev, S.A. Comparison of the Performance and Durability of PEM Fuel Cells with Different Pt-Activated Microporous Layers. *Int. J. Hydrogen Energy* **2021**, *46*, 18093–18106. [CrossRef]
83. Gribov, E.N.; Kuznetsov, A.N.; Golovin, V.A.; Krasnikov, D.V.; Kuznetsov, V.L. Effect of Modification of Multi-Walled Carbon Nanotubes with Nitrogen-Containing Polymers on the Electrochemical Performance of Pt/CNT Catalysts in PEMFC. *Mater. Renew. Sustain. Energy* **2019**, *8*, 7. [CrossRef]
84. Huda, M.; Kawahara, T.; Park, J.-H.; Kawasumi, M.; Matsuo, Y. Single-Walled Carbon Nanotubes Supported Pt Electrocatalyst as a Cathode Catalyst of a Single Fuel Cell with High Durability against Start-up/Shut-down Potential Cycling. *ACS Appl. Energy Mater.* **2023**, *6*, 12226–12236. [CrossRef]
85. Pandia, R.M.; Berchmans, S. Electrochemically Activated Platinum Nanoparticles Trapped by Carbon Nanotubes for Methanol Oxidation Reaction. *J. Electroanal. Chem.* **2023**, *940*, 117492. [CrossRef]
86. Yao, Y.; Izumi, R.; Tsuda, T.; Oshima, Y.; Imanishi, A.; Oda, N.; Kuwabata, S. Platinum and PtNi Nanoparticle-Supported Multiwalled Carbon Nanotube Electrocatalysts Prepared by One-Pot Pyrolytic Synthesis with an Ionic Liquid. *ACS Appl. Energy Mater.* **2019**, *2*, 4865–4872. [CrossRef]
87. Mensharapov, R.M.; Ivanova, N.A.; Zasypkina, A.A.; Spasov, D.D.; Sinyakov, M.V.; Grigoriev, S.A.; Fateev, V.N. Model Study of CNT-Based PEMFCs' Electrocatalytic Layers. *Catalysts* **2022**, *12*, 1227. [CrossRef]
88. Kanninen, P.; Eriksson, B.; Davodi, F.; Buan, M.E.M.; Sorsa, O.; Kallio, T.; Lindström, R.W. Carbon Corrosion Properties and Performance of Multi-Walled Carbon Nanotube Support with and without Nitrogen-Functionalization in Fuel Cell Electrodes. *Electrochim. Acta* **2020**, *332*, 135384. [CrossRef]
89. Kim, J.; Kim, H.; Song, H.; Kim, D.; Kim, G.H.; Im, D.; Jeong, Y.; Park, T. Carbon Nanotube Sheet as a Microporous Layer for Proton Exchange Membrane Fuel Cells. *Energy* **2021**, *227*, 120459. [CrossRef]
90. Zhang, X.-F.; Liu, Y.-T.; Song, H.; Yao, T.-T.; Liu, Q.; Wu, G.-P. Single-Walled Carbon Nanotube Interlayer Modified Gas Diffusion Layers to Boost the Cell Performance of Self-Humidifying Proton Exchange Membrane Fuel Cells. *Int. J. Hydrogen Energy* **2023**, *48*, 30899–30908. [CrossRef]
91. Xi, J.; Meng, K.; Li, Y.; Wang, M.; Liao, Q.; Wei, Z.; Shao, M.; Wang, J. Performance Improvement of Ultra-Low Pt Proton Exchange Membrane Fuel Cell by Catalyst Layer Structure Optimization. *Chin. J. Chem. Eng.* **2022**, *41*, 473–479. [CrossRef]
92. Lee, J.H.; Kim, H.-S.; Yun, E.-T.; Ham, S.-Y.; Park, J.-H.; Ahn, C.H.; Lee, S.H.; Park, H.-D. Vertically Aligned Carbon Nanotube Membranes: Water Purification and Beyond. *Membranes* **2020**, *10*, 273. [CrossRef]
93. Zanin, H.; May, P.W.; Harniman, R.L.; Risbridger, T.; Corat, E.J.; Fermin, D.J. High Surface Area Diamond-like Carbon Electrodes Grown on Vertically Aligned Carbon Nanotubes. *Carbon* **2015**, *82*, 288–296. [CrossRef]
94. Cho, W.; Schulz, M.; Shanov, V. Growth and Characterization of Vertically Aligned Centimeter Long CNT Arrays. *Carbon* **2014**, *72*, 264–273. [CrossRef]
95. Kudinova, E.S.; Vorobyeva, E.A.; Ivanova, N.A.; Tishkin, V.V.; Alekseeva, O.K. A Magnetron Sputtering Method for the Application of the Ni Catalyst for the Synthesis Process of Carbon Nanotube Arrays. *Nanotechnologies Russ.* **2020**, *15*, 715–722. [CrossRef]
96. Ageev, O.A.; Blinov, Y.F.; Il'ina, M.V.; Il'in, O.I.; Smirnov, V.A.; Tsukanova, O.G. Study of Adhesion of Vertically Aligned Carbon Nanotubes to a Substrate by Atomic-Force Microscopy. *Phys. Solid State* **2016**, *58*, 309–314. [CrossRef]
97. Meng, Q.H.; Hao, C.; Yan, B.; Yang, B.; Liu, J.; Shen, P.K.; Tian, Z.Q. High-Performance Proton Exchange Membrane Fuel Cell with Ultra-Low Loading Pt on Vertically Aligned Carbon Nanotubes as Integrated Catalyst Layer. *J. Energy Chem.* **2022**, *71*, 497–506. [CrossRef]
98. Meng, X.; Deng, X.; Zhou, L.; Hu, B.; Tan, W.; Zhou, W.; Liu, M.; Shao, Z. A Highly Ordered Hydrophilic–Hydrophobic Janus Bi-Functional Layer with Ultralow Pt Loading and Fast Gas/Water Transport for Fuel Cells. *Energy Env. Mater.* **2021**, *4*, 126–133. [CrossRef]

99. Lu, C.; Shi, F.; Jin, J.; Peng, X. Study on the Properties of Vertical Carbon Nanotube Films Grown on Stainless Steel Bipolar Plates. *Materials* **2019**, *12*, 899. [CrossRef]

100. Murata, S.; Imanishi, M.; Hasegawa, S.; Namba, R. Vertically Aligned Carbon Nanotube Electrodes for High Current Density Operating Proton Exchange Membrane Fuel Cells. *J. Power Sources* **2014**, *253*, 104–113. [CrossRef]

101. Fontana, M.; Ramos, R.; Morin, A.; Dijon, J. Direct Growth of Carbon Nanotubes Forests on Carbon Fibers to Replace Microporous Layers in Proton Exchange Membrane Fuel Cells. *Carbon* **2021**, *172*, 762–771. [CrossRef]

102. Valdés-Madrigal, M.A.; Montejo-Alvaro, F.; Cernas-Ruiz, A.S.; Rojas-Chávez, H.; Román-Doval, R.; Cruz-Martinez, H.; Medina, D.I. Role of Defect Engineering and Surface Functionalization in the Design of Carbon Nanotube-Based Nitrogen Oxide Sensors. *IJMS* **2021**, *22*, 12968. [CrossRef] [PubMed]

103. Zheng, J.-S.; Zhang, X.-S.; Li, P.; Zhu, J.; Zhou, X.-G.; Yuan, W.-K. Effect of Carbon Nanofiber Microstructure on Oxygen Reduction Activity of Supported Palladium Electrocatalyst. *Electrochem. Commun.* **2007**, *9*, 895–900. [CrossRef]

104. Lavagna, L.; Nisticò, R.; Musso, S.; Pavese, M. Functionalization as a Way to Enhance Dispersion of Carbon Nanotubes in Matrices: A Review. *Mater. Today Chem.* **2021**, *20*, 100477. [CrossRef]

105. Balasubramanian, K.; Burghard, M. Chemically Functionalized Carbon Nanotubes. *Small* **2005**, *1*, 180–192. [CrossRef] [PubMed]

106. Banerjee, S.; Kahn, M.G.C.; Wong, S.S. Rational Chemical Strategies for Carbon Nanotube Functionalization. *Chem. A Eur. J* **2003**, *9*, 1898–1908. [CrossRef] [PubMed]

107. Samad, S.; Loh, K.S.; Wong, W.Y.; Lee, T.K.; Sunarso, J.; Chong, S.T.; Wan Daud, W.R. Carbon and Non-Carbon Support Materials for Platinum-Based Catalysts in Fuel Cells. *Int. J. Hydrogen Energy* **2018**, *43*, 7823–7854. [CrossRef]

108. Meng, L.; Fu, C.; Lu, Q. Advanced Technology for Functionalization of Carbon Nanotubes. *Prog. Nat. Sci.* **2009**, *19*, 801–810. [CrossRef]

109. Hernández-Fernández, P.; Montiel, M.; Ocón, P.; De La Fuente, J.L.G.; García-Rodríguez, S.; Rojas, S.; Fierro, J.L.G. Functionalization of Multi-Walled Carbon Nanotubes and Application as Supports for Electrocatalysts in Proton-Exchange Membrane Fuel Cell. *Appl. Catal. B Environ.* **2010**, *99*, 343–352. [CrossRef]

110. Chen, S.; Wei, Z.; Guo, L.; Ding, W.; Dong, L.; Shen, P.; Qi, X.; Li, L. Enhanced Dispersion and Durability of Pt Nanoparticles on a Thiolated CNT Support. *Chem. Commun.* **2011**, *47*, 10984. [CrossRef]

111. Shaheen Shah, S.; Abu Nayem, S.M.; Sultana, N.; Saleh Ahammad, A.J.; Aziz, M.A. Preparation of Sulfur-doped Carbon for Supercapacitor Applications: A Review. *ChemSusChem* **2022**, *15*, e202101282. [CrossRef]

112. Shirzadi Jahromi, H.; Saxena, S.; Sridhar, S.; Ghantasala, M.K.; Guda, R.; Rozhkova, E.A. Development of Nickel-ZIF-8 Doped Nitrogen Reduced Graphene Oxide Catalytic Materials for PEM Fuel Cell. In Proceedings of the ASME International Mechanical Engineering Congress and Exposition, New Orleans, LA, USA, 29 October 2023; Energy. American Society of Mechanical Engineers: New York, NY, USA, 2023; Volume 7, p. V007T08A045.

113. Bhaskaran, R.; Chetty, R. One-Pot Room Temperature Synthesis of Nitrogen-Doped Graphene and Its Application as Catalyst Support for ORR in PEMFCs. *ACS Appl. Energy Mater.* **2024**, *7*, 390–402. [CrossRef]

114. Lin, Y.-J.; Tsai, J.-E.; Huang, C.-C.; Chen, Y.-S.; Li, Y.-Y. Highly Porous Iron-Doped Nitrogen–Carbon Framework on Reduced Graphene Oxide as an Excellent Oxygen Reduction Catalyst for Proton-Exchange Membrane Fuel Cells. *ACS Appl. Energy Mater.* **2022**, *5*, 1822–1832. [CrossRef]

115. Nair, A.S.; Jafri, R.I. A Facile One-Step Microwave Synthesis of Pt Deposited on N & P Co-Doped Graphene Intercalated Carbon Black—An Efficient Cathode Electrocatalyst for PEM Fuel Cell. *Int. J. Hydrogen Energy* **2023**, *48*, 3653–3664. [CrossRef]

116. Han, C.; Chen, Z. Study on the Synergism of Thermal Transport and Electrochemical of PEMFC Based on N, P Co-Doped Graphene Substrate Electrode. *Energy* **2021**, *214*, 118808. [CrossRef]

117. Peera, S.G.; Menon, R.S.; Das, S.K.; Alfantazi, A.; Karuppasamy, K.; Liu, C.; Sahu, A.K. Oxygen Reduction Electrochemistry at F Doped Carbons: A Review on the Effect of Highly Polarized C-F Bonding in Catalysis and Stability of Fuel Cell Catalysts. *Coord. Chem. Rev.* **2024**, *500*, 215491. [CrossRef]

118. Spasov, D.D.; Ivanova, N.A.; Mensharapov, R.M.; Sinyakov, M.V.; Zasypkina, A.A.; Kukueva, E.V.; Trigub, A.L.; Kulikova, E.S.; Fateev, V.N. Study of the Cathode Pt-Electrocatalysts Based on Reduced Graphene Oxide with Pt-SnO2 Hetero-Clusters. *Inorganics* **2023**, *11*, 325. [CrossRef]

119. Ivanova, N.A.; Spasov, D.D.; Mensharapov, R.M.; Kukueva, E.V.; Zasypkina, A.A.; Fateev, V.N.; Grigoriev, S.A. Efficient and Stable Subzero Operation of a PEM Fuel Cell with a Composite Anode Using Hydrogen-Methanol Composition during Freeze/Thaw Cycles. *Int. J. Hydrogen Energy* **2023**, *48*, 11410–11420. [CrossRef]

120. Wang, R.; Li, X.; Li, H.; Wang, Q.; Wang, H.; Wang, W.; Kang, J.; Chang, Y.; Lei, Z. Highly Stable and Effective Pt/Carbon Nitride (CNx) Modified SiO2 Electrocatalyst for Oxygen Reduction Reaction. *Int. J. Hydrogen Energy* **2011**, *36*, 5775–5781. [CrossRef]

121. Ramírez-Palma, M.T.; Hernández-Padrón, G.; Gómez, J.M.; Rojas-González, F.; Castaño, V.M. NANOSTRUCTURED EPOXY-BASED ANTICORROSIVE COATINGS. *Surf. Rev. Lett.* **2020**, *27*, 1950202. [CrossRef]

122. Chowdury, M.S.K.; Cho, Y.J.; Park, S.B.; Lee, M.H.; Park, Y. Pt-Free Graphene Oxide-Hydrogen Membrane Fuel Cells (GOHMFCs). *Mater. Today Chem.* **2023**, *34*, 101770. [CrossRef]

123. Marinoiu, A.; Raceanu, M.; Carcadea, E.; Varlam, M. Nitrogen-Doped Graphene Oxide as Efficient Metal-Free Electrocatalyst in PEM Fuel Cells. *Nanomaterials* **2023**, *13*, 1233. [CrossRef] [PubMed]

124. Min, H.; Choi, J.-H.; Kang, H.E.; Kim, D.-J.; Yoon, Y.S. Enhanced Durability and Catalytic Performance of Pt–SnO$_2$ /Multi-Walled Carbon Nanotube with Shifted d-Band Center for Proton-Exchange Membrane Fuel Cells. *Small Struct.* **2024**, *5*, 2300407. [CrossRef]

125. Hoque, M.A.; Hassan, F.M.; Jauhar, A.M.; Jiang, G.; Pritzker, M.; Choi, J.-Y.; Knights, S.; Ye, S.; Chen, Z. Web-like 3D Architecture of Pt Nanowires and Sulfur-Doped Carbon Nanotube with Superior Electrocatalytic Performance. *ACS Sustain. Chem. Eng.* **2018**, *6*, 93–98. [CrossRef]

126. Lu, L.; Deng, H.; Zhao, Z.; Xu, B.; Sun, X. N-Doped Carbon Nanotubes Supported Pt Nanowire Catalysts for Proton Exchange Membrane Fuel Cells. *J. Power Sources* **2022**, *529*, 231229. [CrossRef]

127. Mardle, P.; Ji, X.; Wu, J.; Guan, S.; Dong, H.; Du, S. Thin Film Electrodes from Pt Nanorods Supported on Aligned N-CNTs for Proton Exchange Membrane Fuel Cells. *Appl. Catal. B Environ.* **2020**, *260*, 118031. [CrossRef]

128. Roudbari, M.N.; Ojani, R.; Raoof, J.B. Nitrogen Functionalized Carbon Nanotubes as a Support of Platinum Electrocatalysts for Performance Improvement of ORR Using Fuel Cell Cathodic Half-Cell. *Renew. Energy* **2020**, *159*, 1015–1028. [CrossRef]

129. Xu, Z.; Zhou, Z.; Li, B.; Wang, G.; Leu, P.W. Identification of Efficient Active Sites in Nitrogen-Doped Carbon Nanotubes for Oxygen Reduction Reaction. *J. Phys. Chem. C* **2020**, *124*, 8689–8696. [CrossRef]

130. Dogan, D.C.; Cho, S.; Hwang, S.-M.; Kim, Y.-M.; Guim, H.; Yang, T.-H.; Park, S.-H.; Park, G.-G.; Yim, S.-D. Highly Durable Supportless Pt Hollow Spheres Designed for Enhanced Oxygen Transport in Cathode Catalyst Layers of Proton Exchange Membrane Fuel Cells. *ACS Appl. Mater. Interfaces* **2016**, *8*, 27730–27739. [CrossRef]

131. Shu, C.; Tan, Q.; Deng, C.; Du, W.; Gan, Z.; Liu, Y.; Fan, C.; Jin, H.; Tang, W.; Yang, X.; et al. Hierarchically Mesoporous Carbon Spheres Coated with a Single Atomic Fe–N–C Layer for Balancing Activity and Mass Transfer in Fuel Cells. *Carbon Energy* **2022**, *4*, 1–11. [CrossRef]

132. Mashindi, V.; Mente, P.; Mpofu, N.; Phaahlamohlaka, T.N.; Makgae, O.; Kirkland, A.I.; Forbes, R.; Ozoemena, K.I.; Levecque, P.B.; Coville, N.J. Platinum Supported on Pristine and Nitrogen-Doped Bowl-like Broken Hollow Carbon Spheres as Oxygen Reduction Reaction Catalysts. *J. Appl. Electrochem.* **2021**, *51*, 991–1008. [CrossRef]

133. Wang, Y.; Tan, G.; Yi, Q.; Fang, C.; Yi, R. N-Doped Hollow Carbon Sphere and Polyhedral Carbon Composite Supported Pt/Fe Nanoparticles as Highly Efficient Cathodic Catalysts of Proton-Exchange Membrane Fuel Cells. *ACS Appl. Energy Mater.* **2023**, *6*, 1228–1238. [CrossRef]

134. Panickar, R.; Sobhan, C.B.; Chakravorti, S. Chemical Vapor Deposition Synthesis of Carbon Spheres: Effects of Temperature and Hydrogen. *Vacuum* **2020**, *172*, 109108. [CrossRef]

135. Kızılduman, B.K.; Turhan, Y.; Doğan, M. Mesoporous Carbon Spheres Produced by Hydrothermal Carbonization from Rice Husk: Optimization, Characterization and Hydrogen Storage. *Adv. Powder Technol.* **2021**, *32*, 4222–4234. [CrossRef]

136. Xu, M.; Yu, Q.; Liu, Z.; Lv, J.; Lian, S.; Hu, B.; Mai, L.; Zhou, L. Tailoring Porous Carbon Spheres for Supercapacitors. *Nanoscale* **2018**, *10*, 21604–21616. [CrossRef] [PubMed]

137. Yu, S.; Dong, X.; Zhao, P.; Luo, Z.; Sun, Z.; Yang, X.; Li, Q.; Wang, L.; Zhang, Y.; Zhou, H. Decoupled Temperature and Pressure Hydrothermal Synthesis of Carbon Sub-Micron Spheres from Cellulose. *Nat. Commun.* **2022**, *13*, 3616. [CrossRef] [PubMed]

138. Mao, H.; Chen, X.; Huang, R.; Chen, M.; Yang, R.; Lan, P.; Zhou, M.; Zhang, F.; Yang, Y.; Zhou, X. Fast Preparation of Carbon Spheres from Enzymatic Hydrolysis Lignin: Effects of Hydrothermal Carbonization Conditions. *Sci. Rep.* **2018**, *8*, 9501. [CrossRef]

139. Yu, Q.; Xu, J.; Wu, C.; Zhang, J.; Guan, L. MnO$_2$ Nanofilms on Nitrogen-Doped Hollow Graphene Spheres as a High-Performance Electrocatalyst for Oxygen Reduction Reaction. *ACS Appl. Mater. Interfaces* **2016**, *8*, 35264–35269. [CrossRef] [PubMed]

140. Navas, D.; Fuentes, S.; Castro-Alvarez, A.; Chavez-Angel, E. Review on Sol-Gel Synthesis of Perovskite and Oxide Nanomaterials. *Gels* **2021**, *7*, 275. [CrossRef]

141. Karimi Estahbanati, M.R.; Feilizadeh, M.; Shokrollahi Yancheshmeh, M.; Iliuta, M.C. Effects of Carbon Nanotube and Carbon Sphere Templates in TiO$_2$ Composites for Photocatalytic Hydrogen Production. *Ind. Eng. Chem. Res.* **2019**, *58*, 2770–2783. [CrossRef]

142. Bokov, D.; Turki Jalil, A.; Chupradit, S.; Suksatan, W.; Javed Ansari, M.; Shewael, I.H.; Valiev, G.H.; Kianfar, E. Nanomaterial by Sol-Gel Method: Synthesis and Application. *Advances in Materials Science and Engineering* **2021**, *2021*, 5102014. [CrossRef]

143. Ebisike, K.; Okoronkwo, A.E.; Alaneme, K.K. Synthesis and Characterization of Chitosan–Silica Hybrid Aerogel Using Sol-Gel Method. *J. King Saud Univ. -Sci.* **2020**, *32*, 550–554. [CrossRef]

144. Ozouf, G.; Cognard, G.; Maillard, F.; Chatenet, M.; Guétaz, L.; Heitzmann, M.; Jacques, P.-A.; Beauger, C. Sb-Doped SnO$_2$ Aerogels Based Catalysts for Proton Exchange Membrane Fuel Cells: Pt Deposition Routes, Electrocatalytic Activity and Durability. *J. Electrochem. Soc.* **2018**, *165*, F3036. [CrossRef]

145. Shen, M.; Qi, J.; Gao, K.; Duan, C.; Liu, J.; Liu, Q.; Yang, H.; Ni, Y. Chemical Vapor Deposition Strategy for Inserting Atomic FeN4 Sites into 3D Porous Honeycomb Carbon Aerogels as Oxygen Reduction Reaction Catalysts in High-Performance Zn-Air Batteries. *Chem. Eng. J.* **2023**, *464*, 142719. [CrossRef]

146. Shaari, N.; Kamarudin, S.K. Current Status, Opportunities, and Challenges in Fuel Cell Catalytic Application of Aerogels. *Int. J. Energy Res.* **2019**, *43*, 2447–2467. [CrossRef]

147. Wang, Y.; Larsen, M.J.; Rojas, S.; Sougrati, M.-T.; Jaouen, F.; Ferrer, P.; Gianolio, D.; Berthon-Fabry, S. Influence of the Synthesis Parameters on the Proton Exchange Membrane Fuel Cells Performance of Fe–N–C Aerogel Catalysts. *J. Power Sources* **2021**, *514*, 230561. [CrossRef]

148. Alwin, S.; Sahaya Shajan, X. Aerogels: Promising Nanostructured Materials for Energy Conversion and Storage Applications. *Mater Renew Sustain. Energy* **2020**, *9*, 7. [CrossRef]

149. Öner, E.; Öztürk, A.; Yurtcan, A.B. Utilization of the Graphene Aerogel as PEM Fuel Cell Catalyst Support: Effect of Polypyrrole (PPy) and Polydimethylsiloxane (PDMS) Addition. *Int. J. Hydrog. Energy* **2020**, *45*, 34818–34836. [CrossRef]

150. Gu, K.; Kim, E.J.; Sharma, S.K.; Sharma, P.R.; Bliznakov, S.; Hsiao, B.S.; Rafailovich, M.H. Mesoporous Carbon Aerogel with Tunable Porosity as the Catalyst Support for Enhanced Proton-Exchange Membrane Fuel Cell Performance. *Mater. Today Energy* **2021**, *19*, 100560. [CrossRef]

151. Pasatoa, C.D.; Lawa, A.; Parka, J.; Kima, M.; Jina, P. The Synthesis of High Surface Area Carbon Aerogels. *J. Undergrad. Chem. Eng. Res* **2020**, *9*, 27–30.

152. Liu, X.; Tian, J.; Zhou, C.; Jiang, J.; Cheng, X.; Yang, L.; Wu, Q.; Wang, X.; Hu, Z. Constructing Membrane Electrodes of Low Pt Areal Loading with the New Support of N-Doped Carbon Nanocages for PEMFC. *FlatChem* **2023**, *40*, 100515. [CrossRef]

153. Kagkoura, A.; Tagmatarchis, N. Carbon Nanohorn-Based Electrocatalysts for Energy Conversion. *Nanomaterials* **2020**, *10*, 1407. [CrossRef] [PubMed]

154. Kausar, A. Polymer/Carbon Nanocoil Nanocomposite: Status and Future Directions. *Polym. -Plast. Technol. Mater.* **2021**, *60*, 816–829. [CrossRef]

155. Yeon, J.H.; Park, S.J.; Choi, I.; Choi, M. Generation of Carbon Nano-Onions by Laser Irradiation of Gaseous Hydrocarbons for High Durability Catalyst Support in Proton Exchange Membrane Fuel Cells. *J. Ind. Eng. Chem.* **2019**, *80*, 65–73. [CrossRef]

156. Yeon, J.H.; Choi, J.; Jang, S.; Choi, M. Hydrophilicity Control of Laser-Induced Amorphous Carbon-Encapsulated Carbon Nano-Onions and Their Application to Proton Exchange Membrane Fuel Cells under Low Humidity. *Carbon* **2021**, *184*, 910–922. [CrossRef]

157. Wu, J.; Sun, Y.-M.; Wu, Z.; Li, X.; Wang, N.; Tao, K.; Wang, G.P. Carbon Nanocoil-Based Fast-Response and Flexible Humidity Sensor for Multifunctional Applications. *ACS Appl. Mater. Interfaces* **2019**, *11*, 4242–4251. [CrossRef]

158. Zuo, X.; Zhao, Y.; Zhang, H.; Huang, H.; Zhou, C.; Cong, T.; Muhammad, J.; Yang, X.; Zhang, Y.; Fan, Z. Surface Modification of Helical Carbon Nanocoil (CNC) with N-Doped and Co-Anchored Carbon Layer for Efficient Microwave Absorption. *J. Colloid Interface Sci.* **2022**, *608*, 1894–1906. [CrossRef] [PubMed]

159. Ma, L.; Bi, Z.; Zhang, W.; Zhang, Z.; Xiao, Y.; Niu, H.; Huang, Y. Synthesis of a Three-Dimensional Interconnected Oxygen-, Boron-, Nitrogen-, and Phosphorus Tetratomic-Doped Porous Carbon Network as Electrode Material for the Construction of a Superior Flexible Supercapacitor. *ACS Appl. Mater. Interfaces* **2020**, *12*, 46170–46180. [CrossRef] [PubMed]

160. Wang, Y.; Luo, S.; Chen, M.; Wu, L. Uniformly Confined Germanium Quantum Dots in 3D Ordered Porous Carbon Framework for High-Performance Li-ion Battery. *Adv. Funct. Mater.* **2020**, *30*, 2000373. [CrossRef]

161. Sam, D.K.; Li, H.; Xu, Y.T.; Cao, Y. Porous Carbon Fabrication Techniques: A Review. *J. Ind. Eng. Chem.* **2024**, *in press*. [CrossRef]